



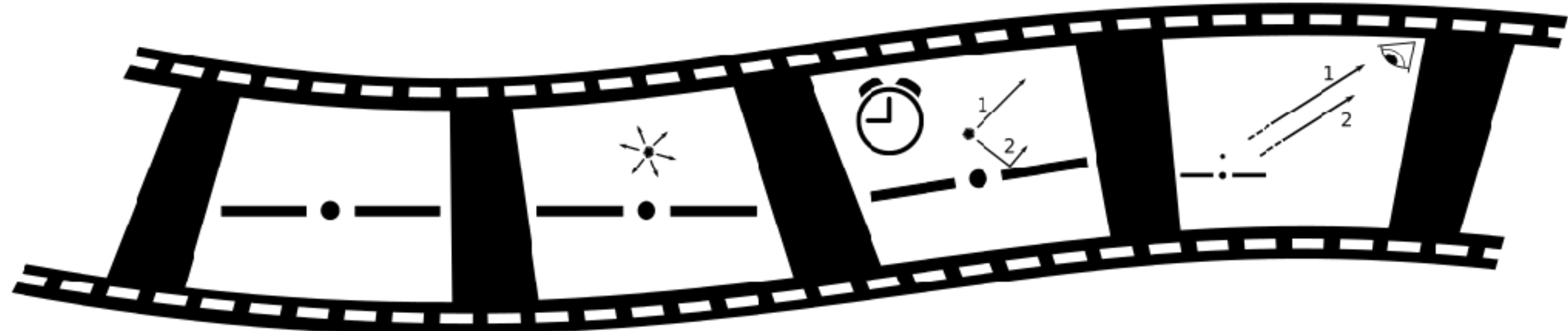
UNIVERSITY OF AMSTERDAM

ANTON PANNEKOEK
INSTITUTE

X-ray Reverberation Mass Measurement of Cygnus X-1

G. Mastroserio

A. Ingram, M. van der Klis



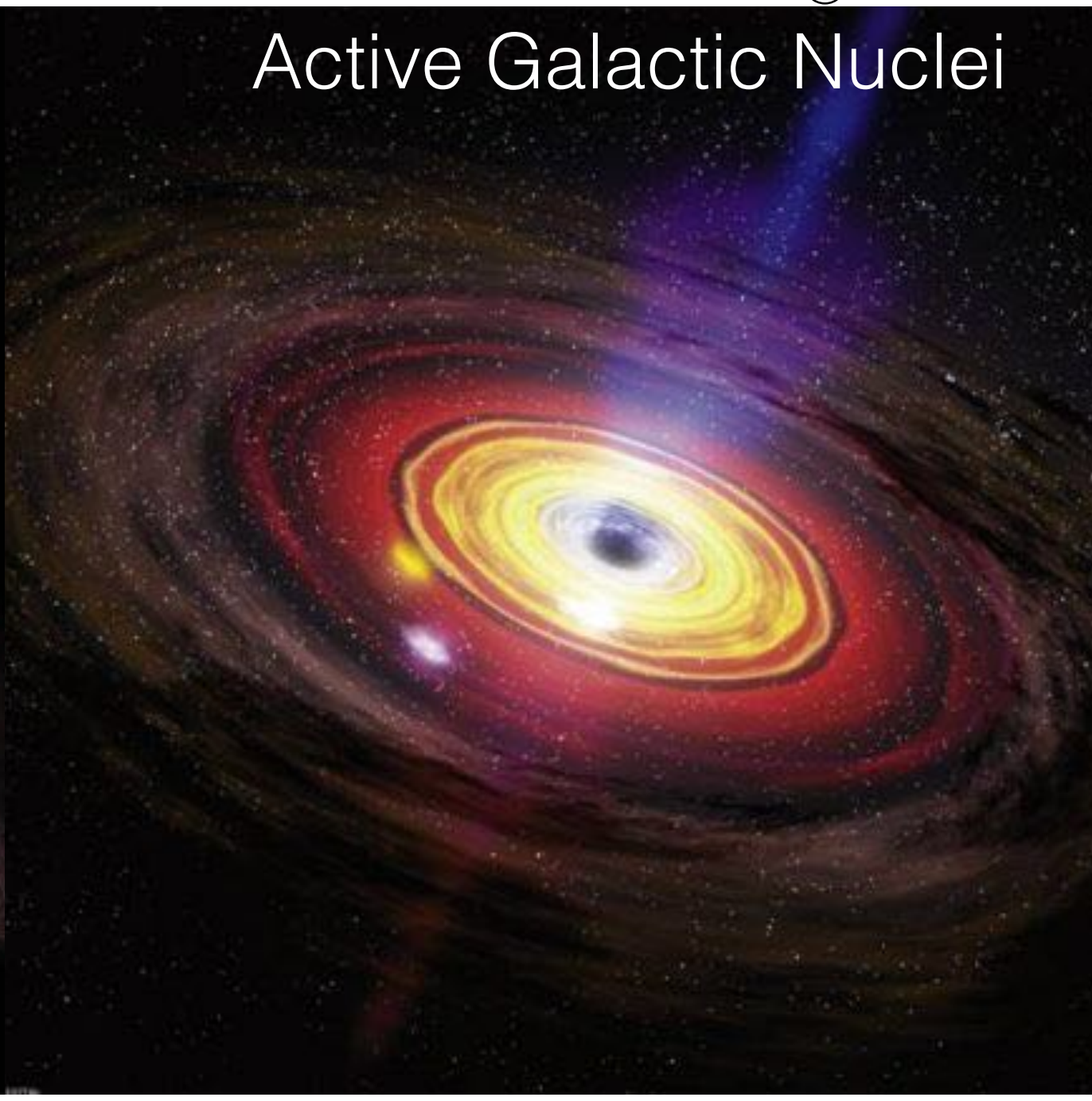
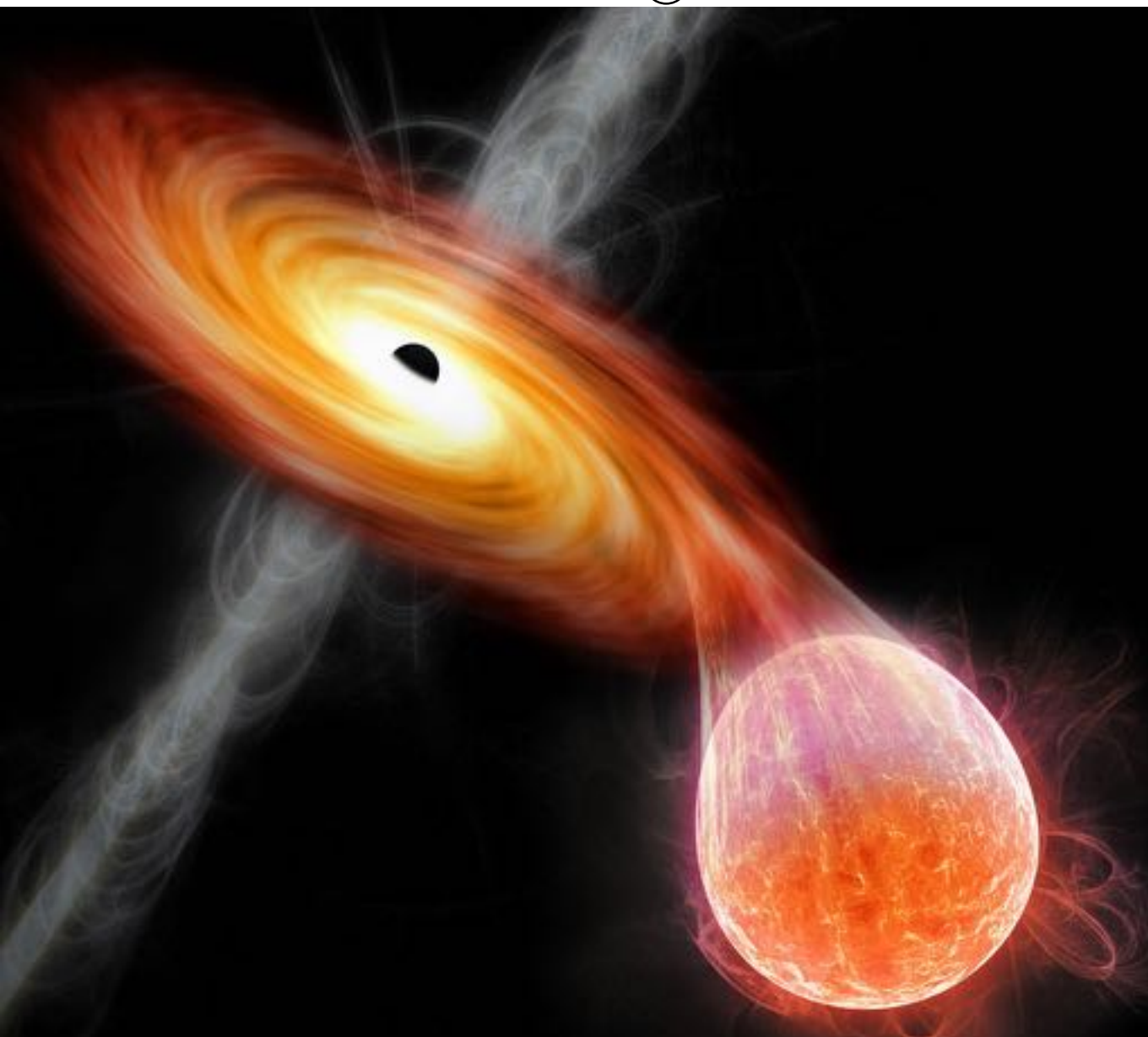
BHBs and AGN

$\sim 10 M_\odot$

Mass

$\sim 10^6 - 10^9 M_\odot$

Active Galactic Nuclei



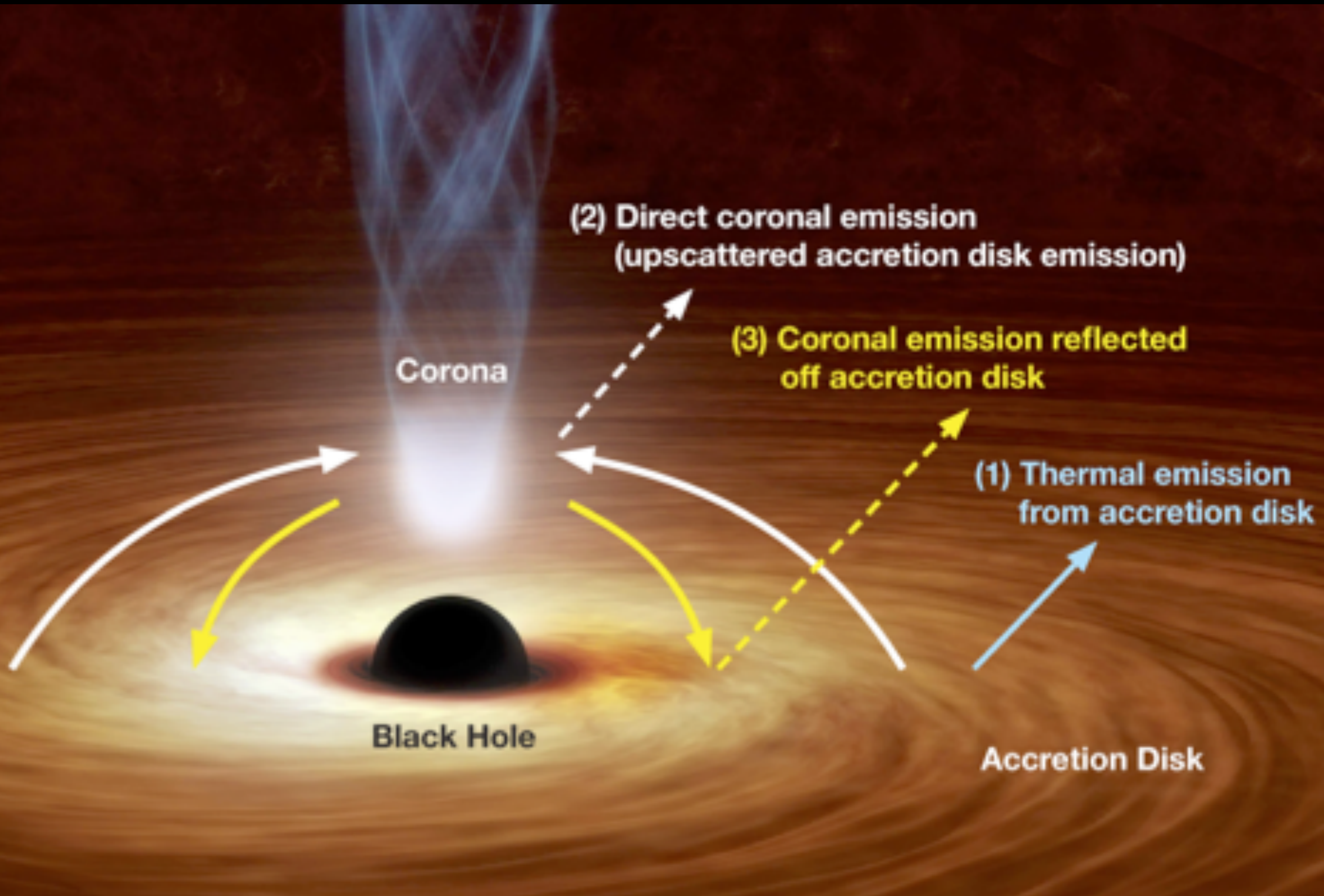
Black Hole Binaries

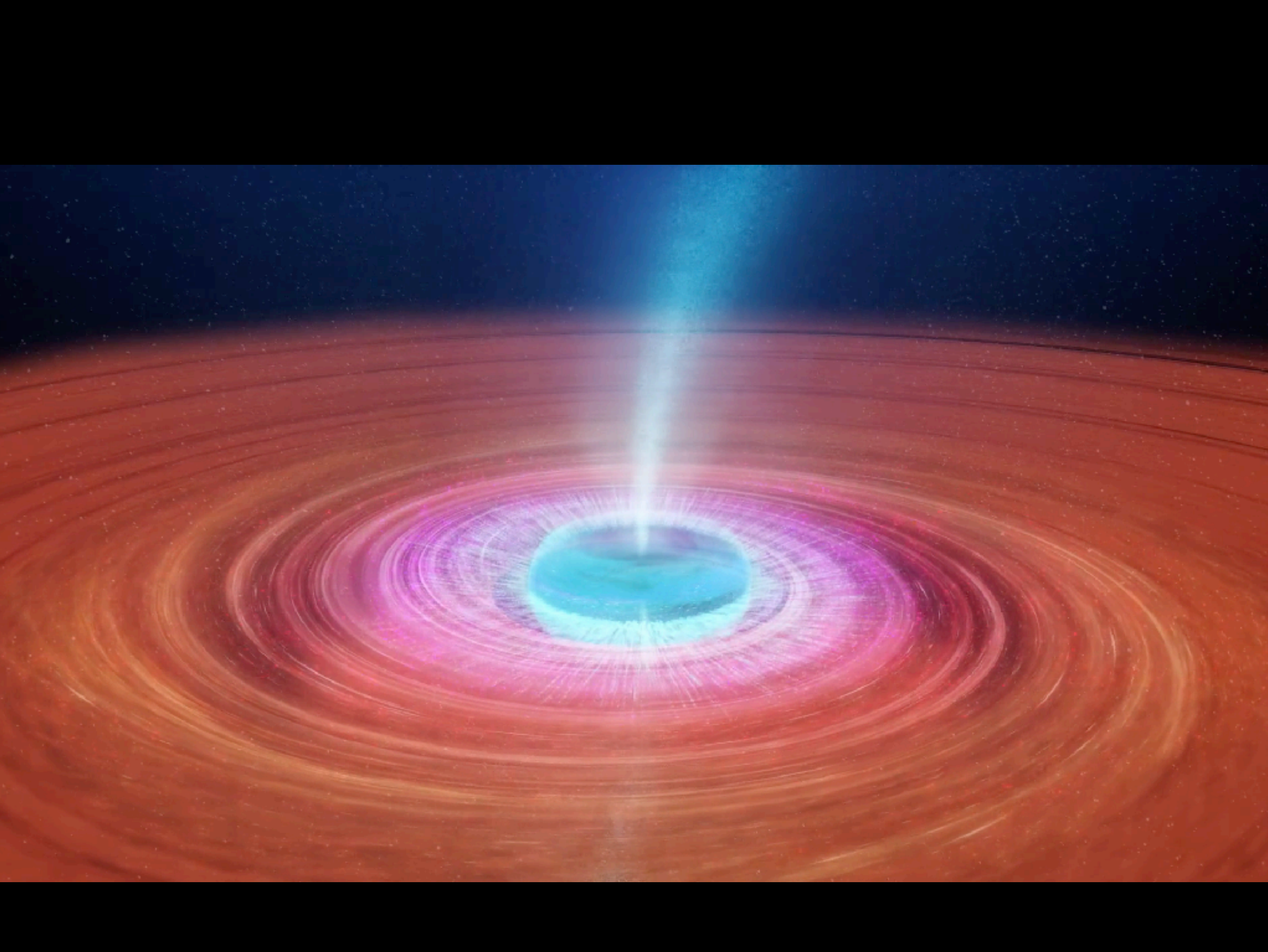
Different mass (!), same central geometry (?)



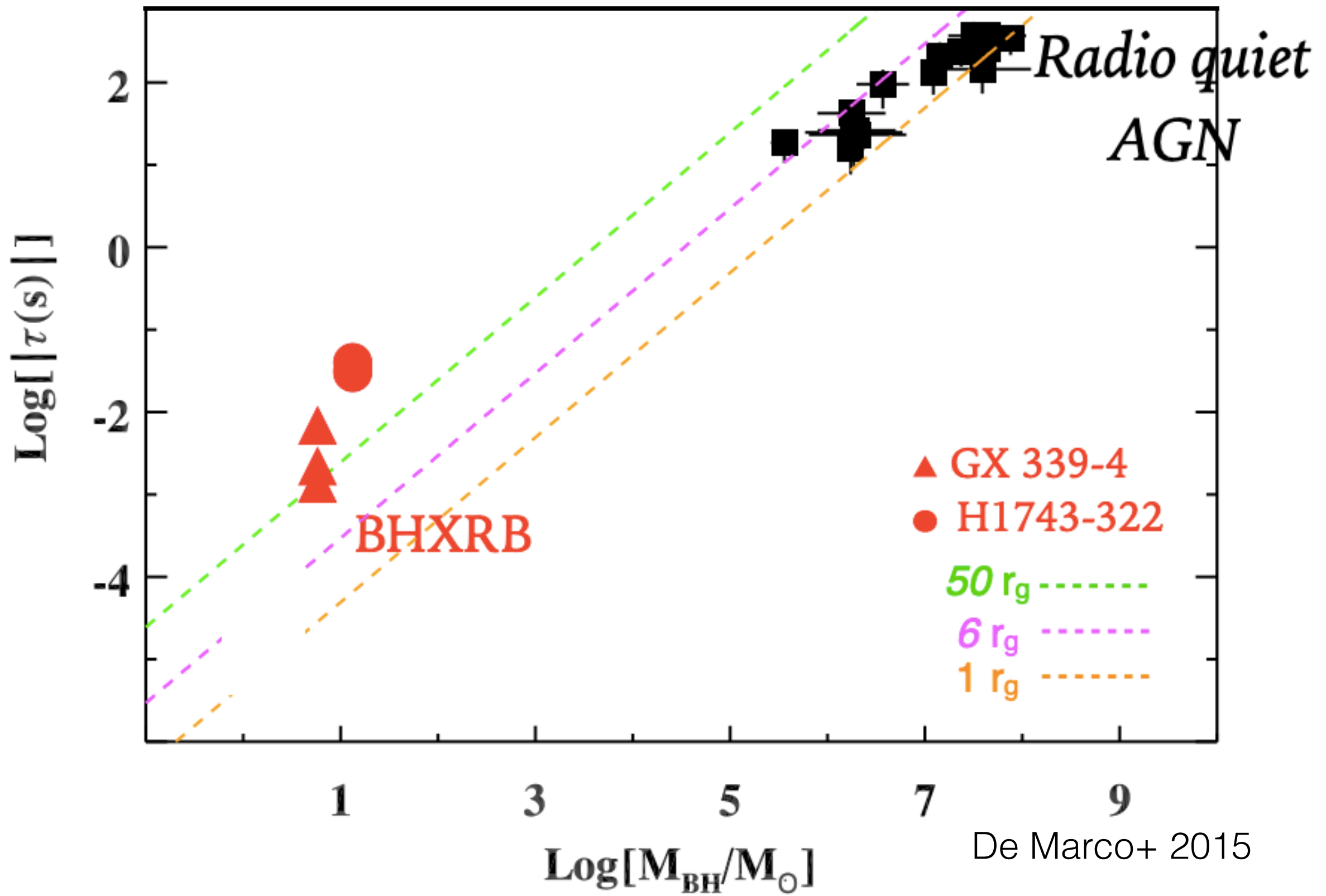
ANTON PANNEKOEK
INSTITUTE

Emission from the system



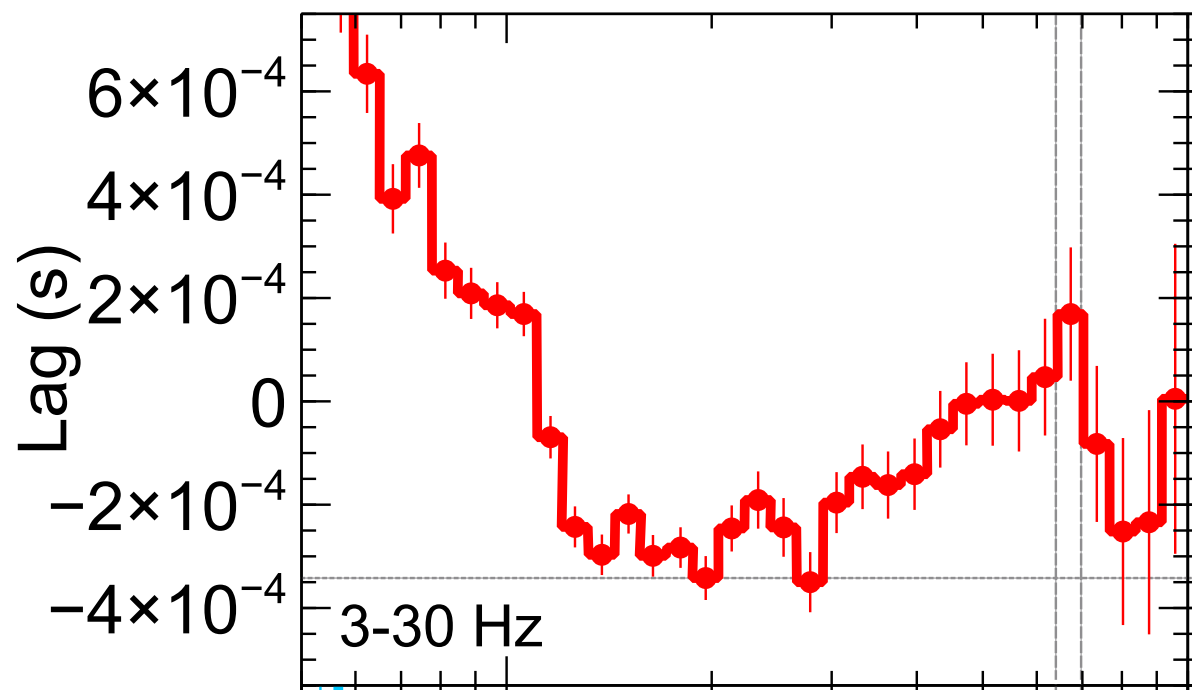
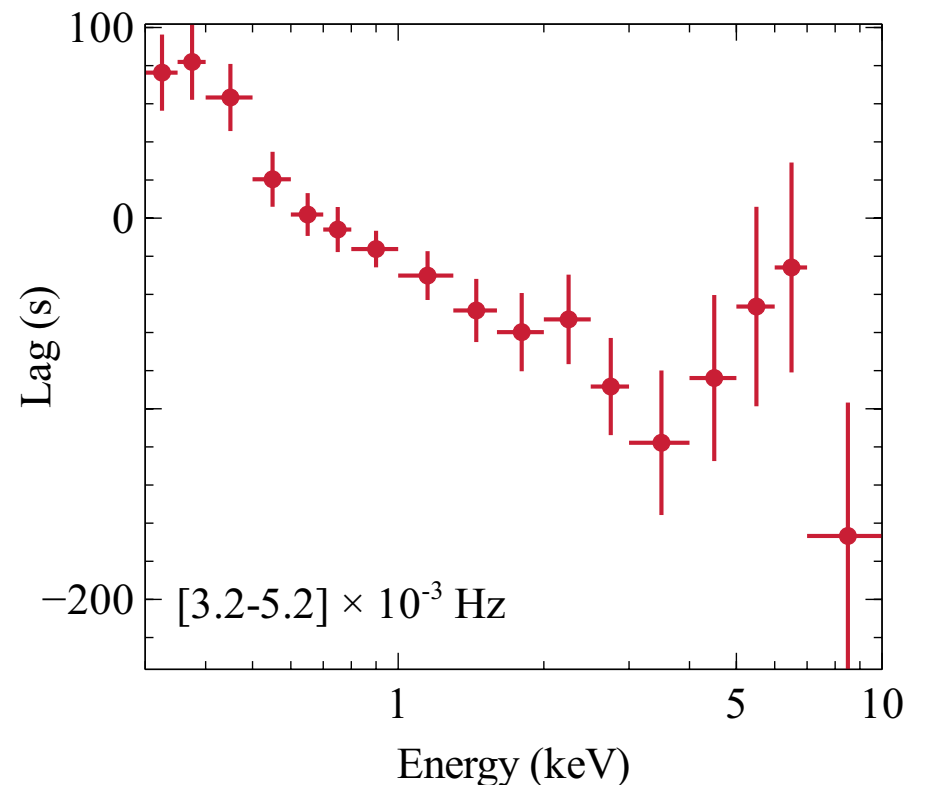


Lag vs BH mass



Lags vs Energy

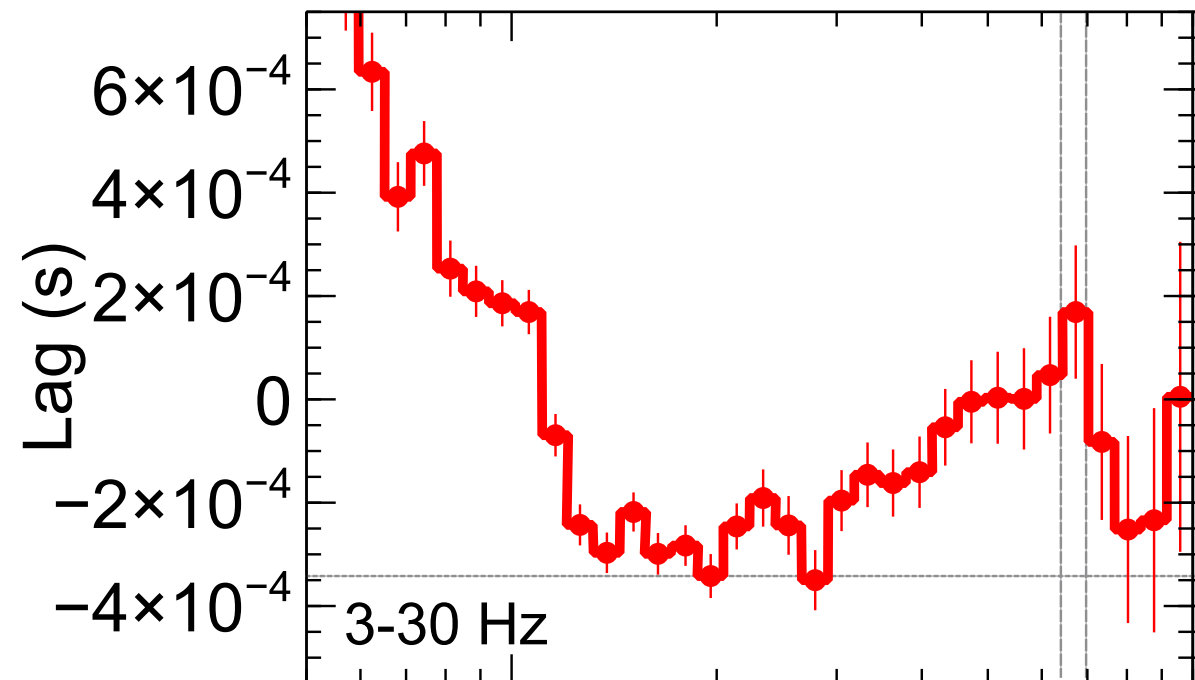
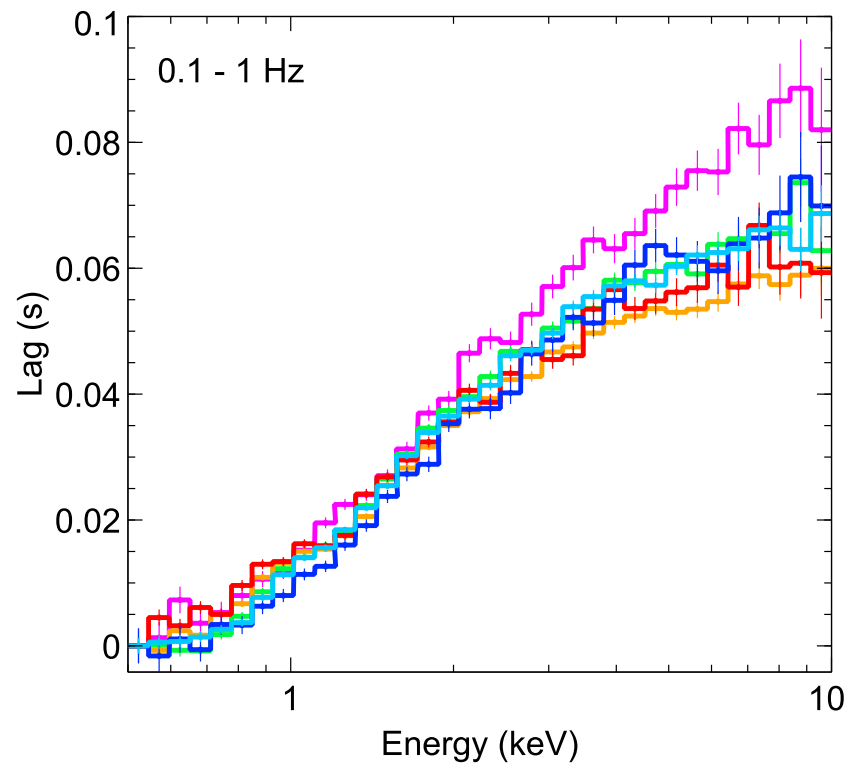
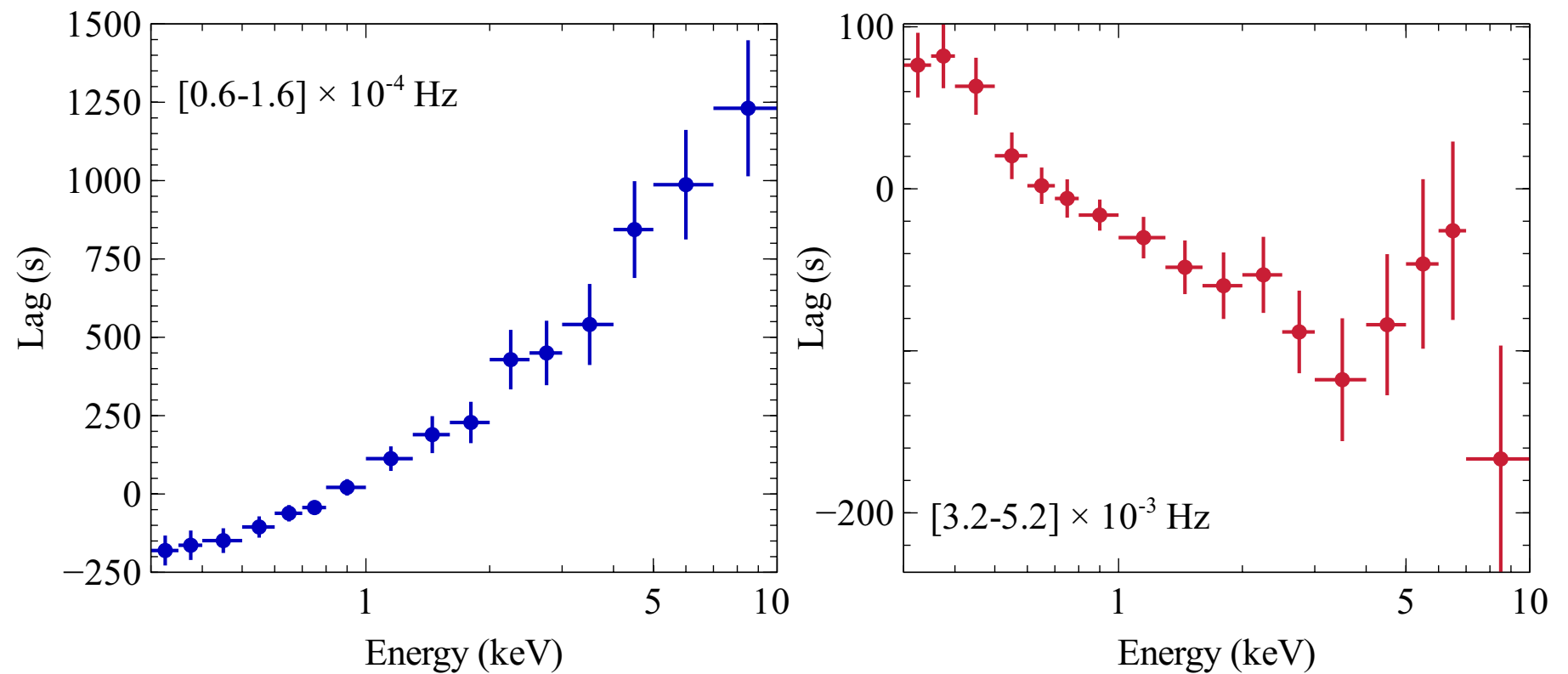
AGN
Ark 564
 $M \simeq 10^6 M_\odot$
Kara+ 2013



BHB
MAXI
J1820+070
 $M \simeq 10M_\odot$
Kara+ 2019

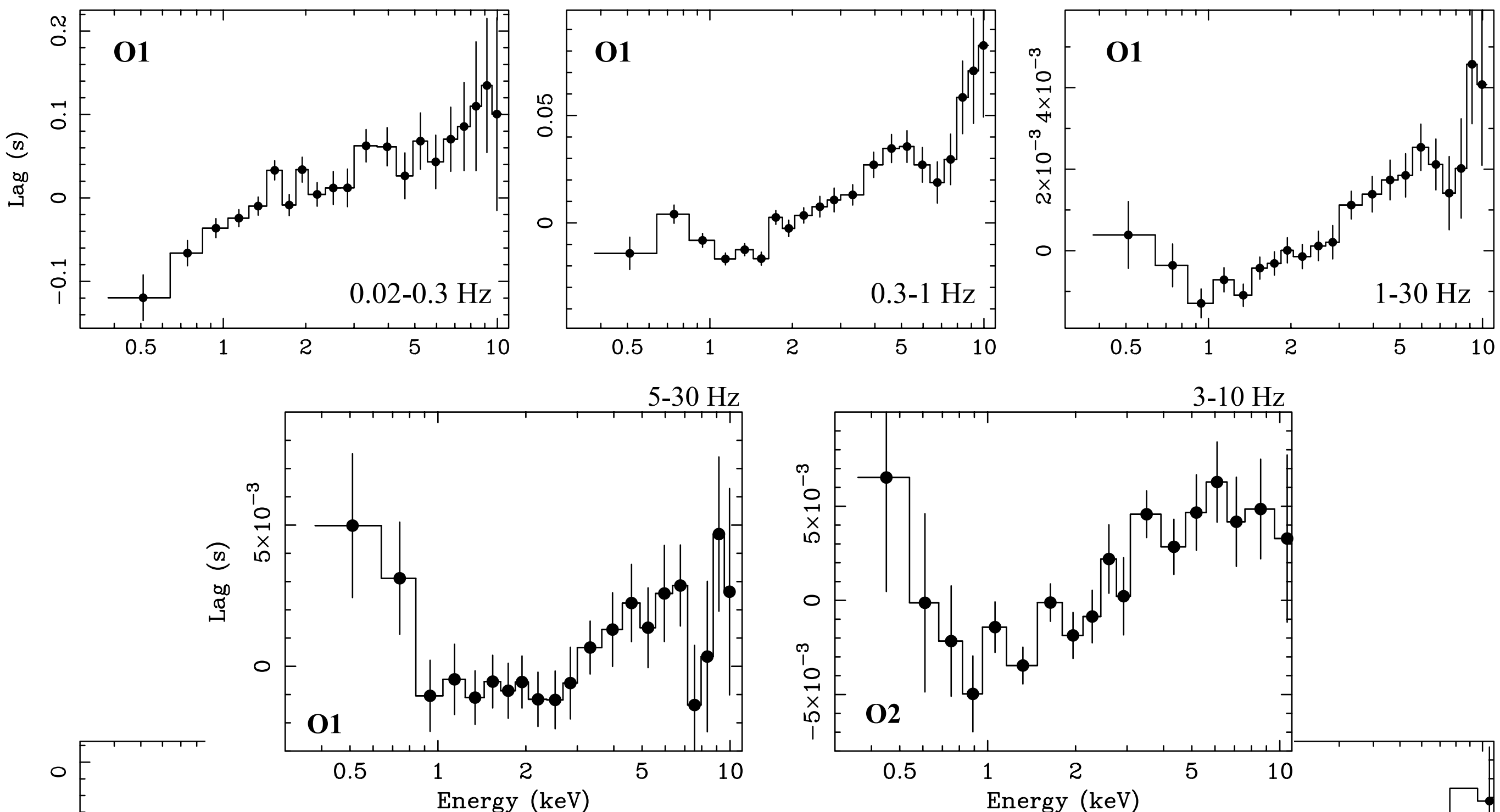
Lags vs Energy

AGN
 Ark 564
 $M \simeq 10^6 M_\odot$
 Kara+ 2013



BHB
 MAXI
 J1820+070
 $M \simeq 10 M_\odot$
 Kara+ 2019

GX 339-4



De Marco+ 2017

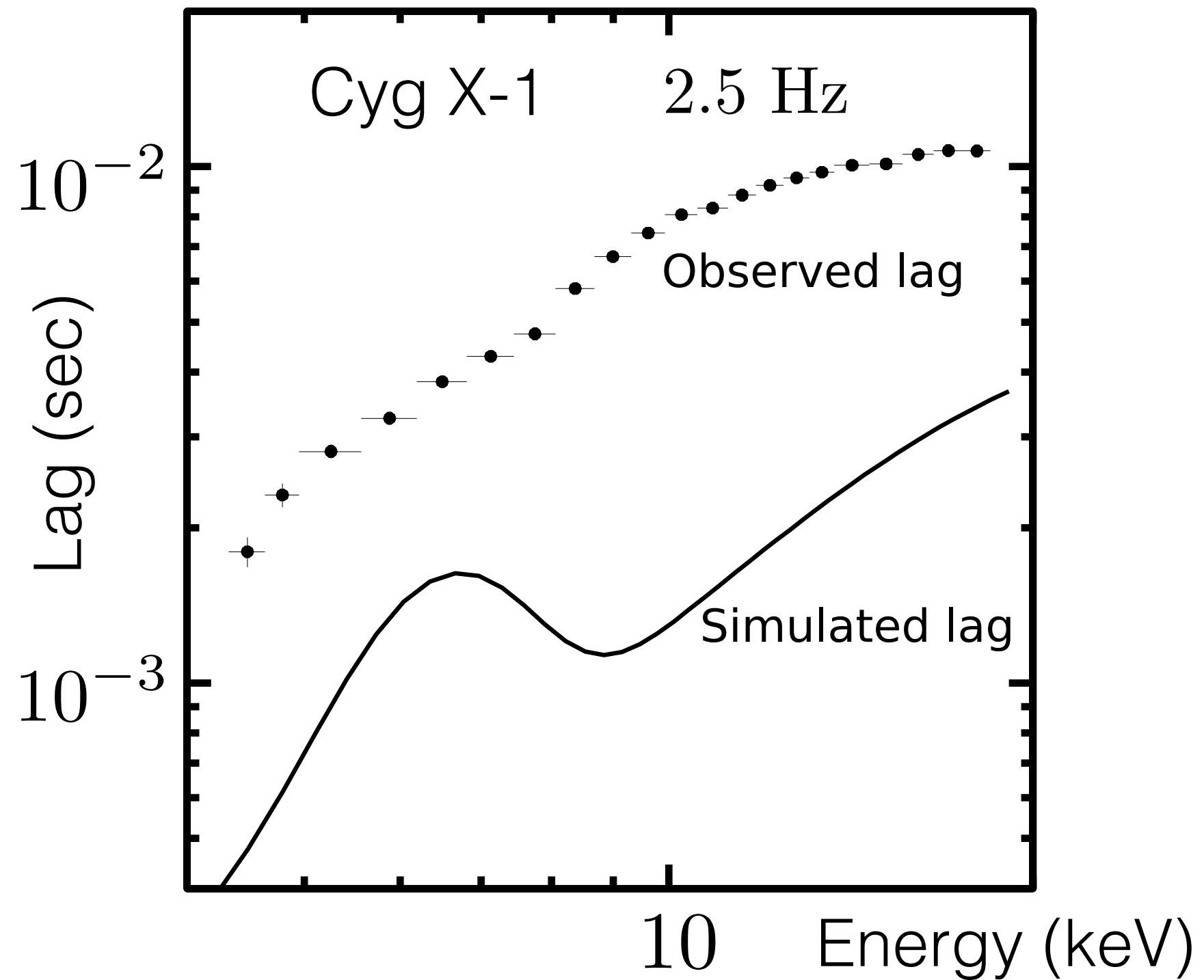


Cygnus X-1

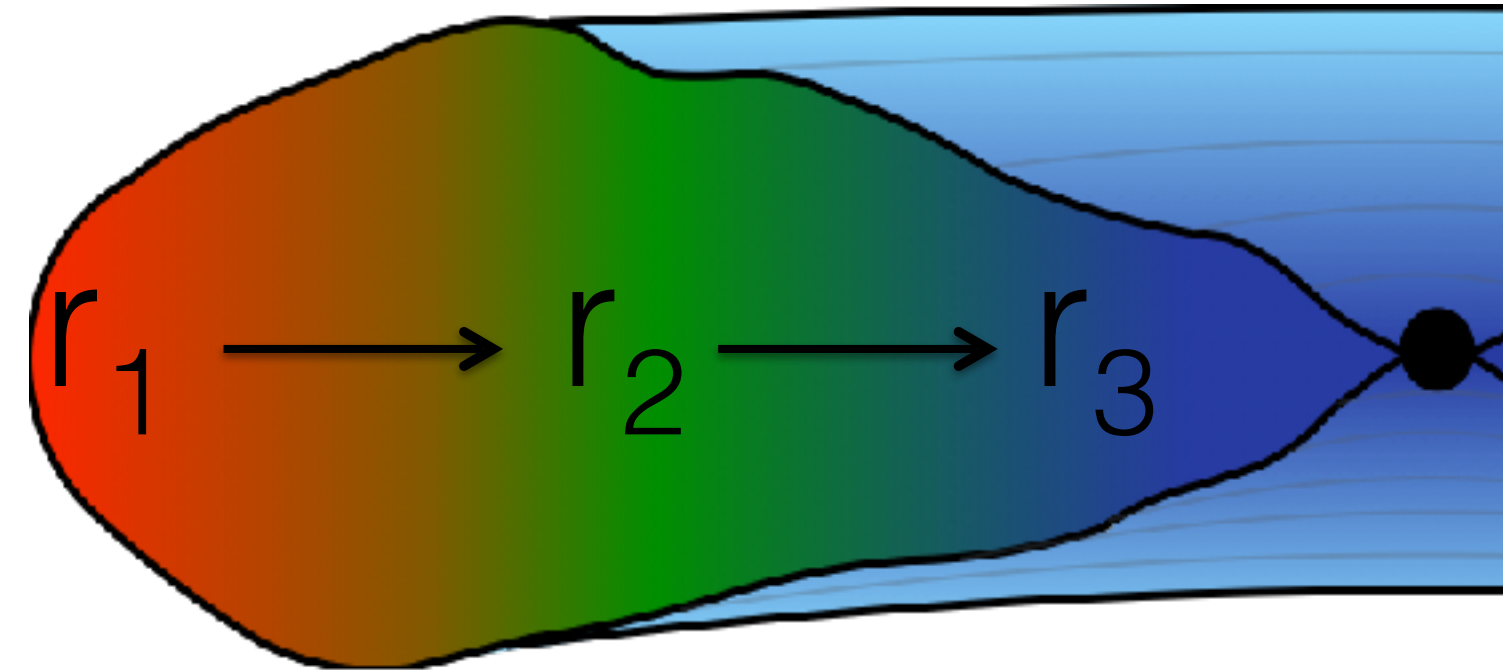
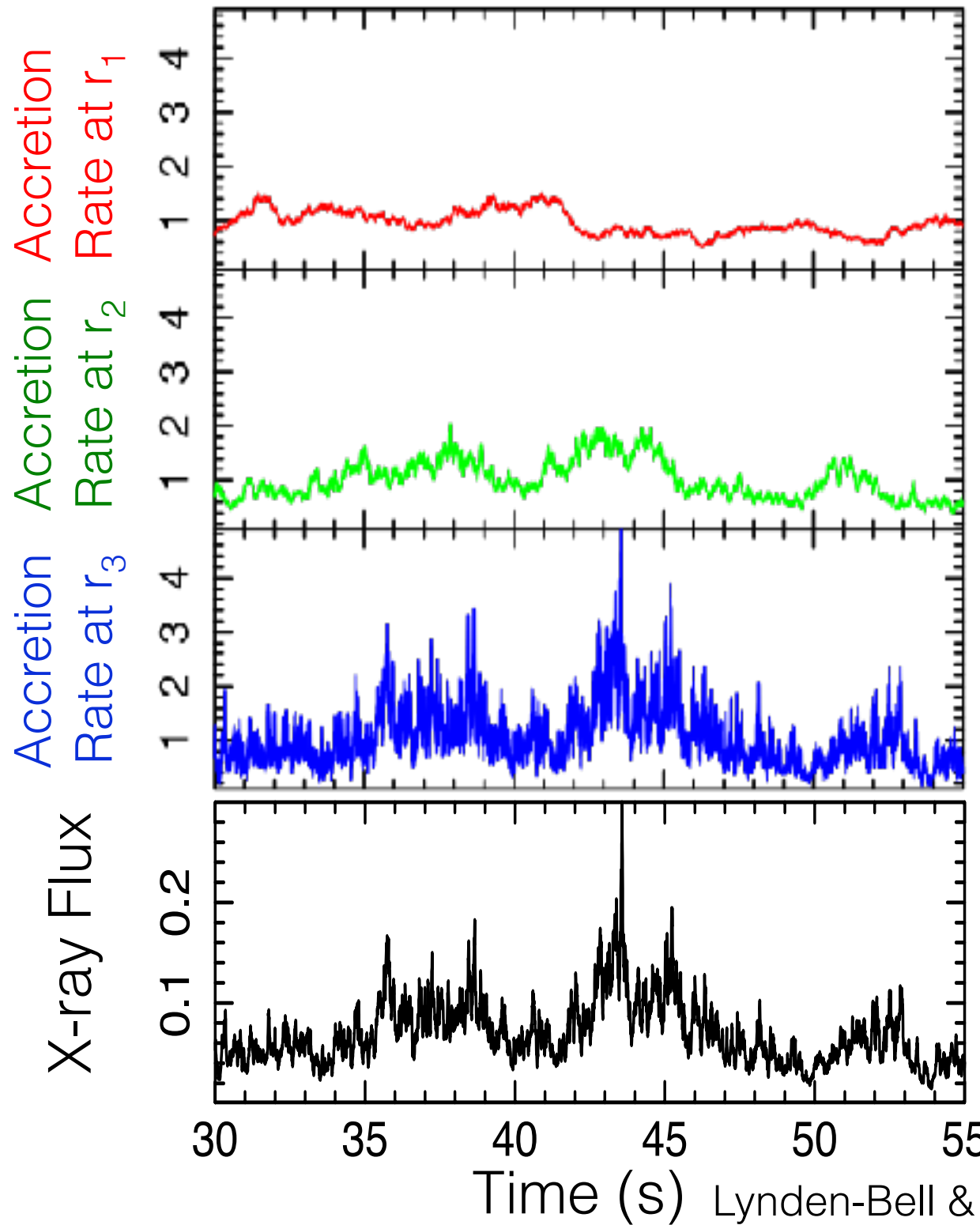
Hard state:
March 1996
(P10238)

Attempt to
reproduce
Cygnus X-1
lags with X-ray
reverberation

Kotov+ 2001



Propagating fluctuations model

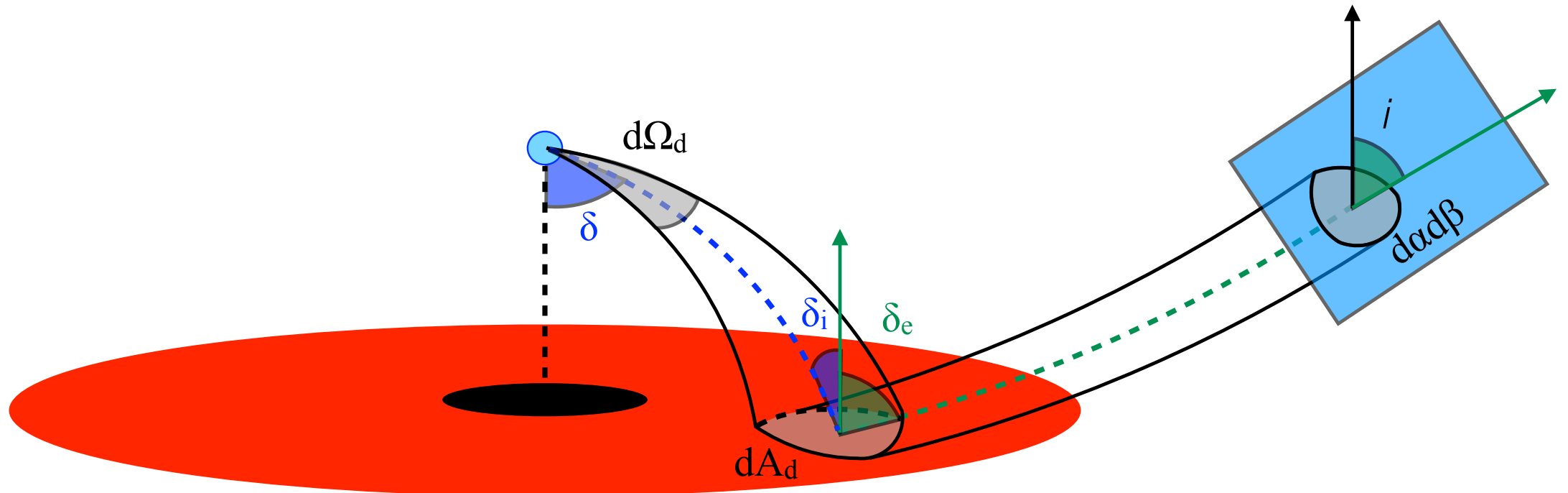


- The variability in the mass accretion rate is limited by the local viscous timescale
- Slow fluctuations originating far from the black hole propagate in to modulate the faster fluctuations

Lynden-Bell & Pringle (1974); Lyubarskii (1997); Arevalo & Uttley (2006)



Reltrans model



- Fully relativistic ray-tracing model
- Different emission angle of the reprocessed radiation
- Different high energy cut off seen by the disc
- Complex cross-spectrum fitting
- Accounting properly for the response matrix

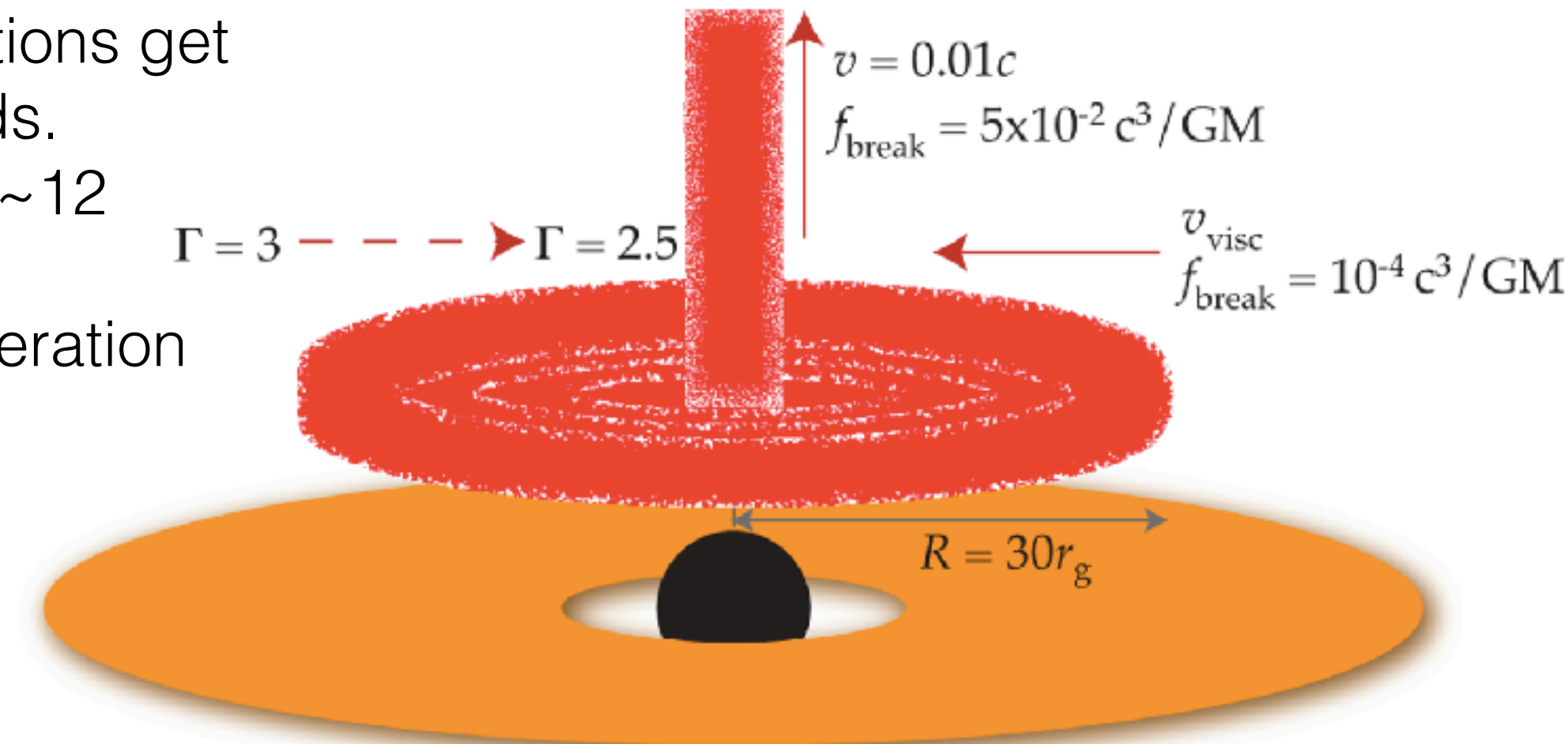
Ingram, Mastroserio+ 2019



Extended Corona

It combines mass accretion rate propagating fluctuations and reverberation

Propagating fluctuations get inwards and upwards.
The model involves ~ 12 transfer functions to calculate the reverberation



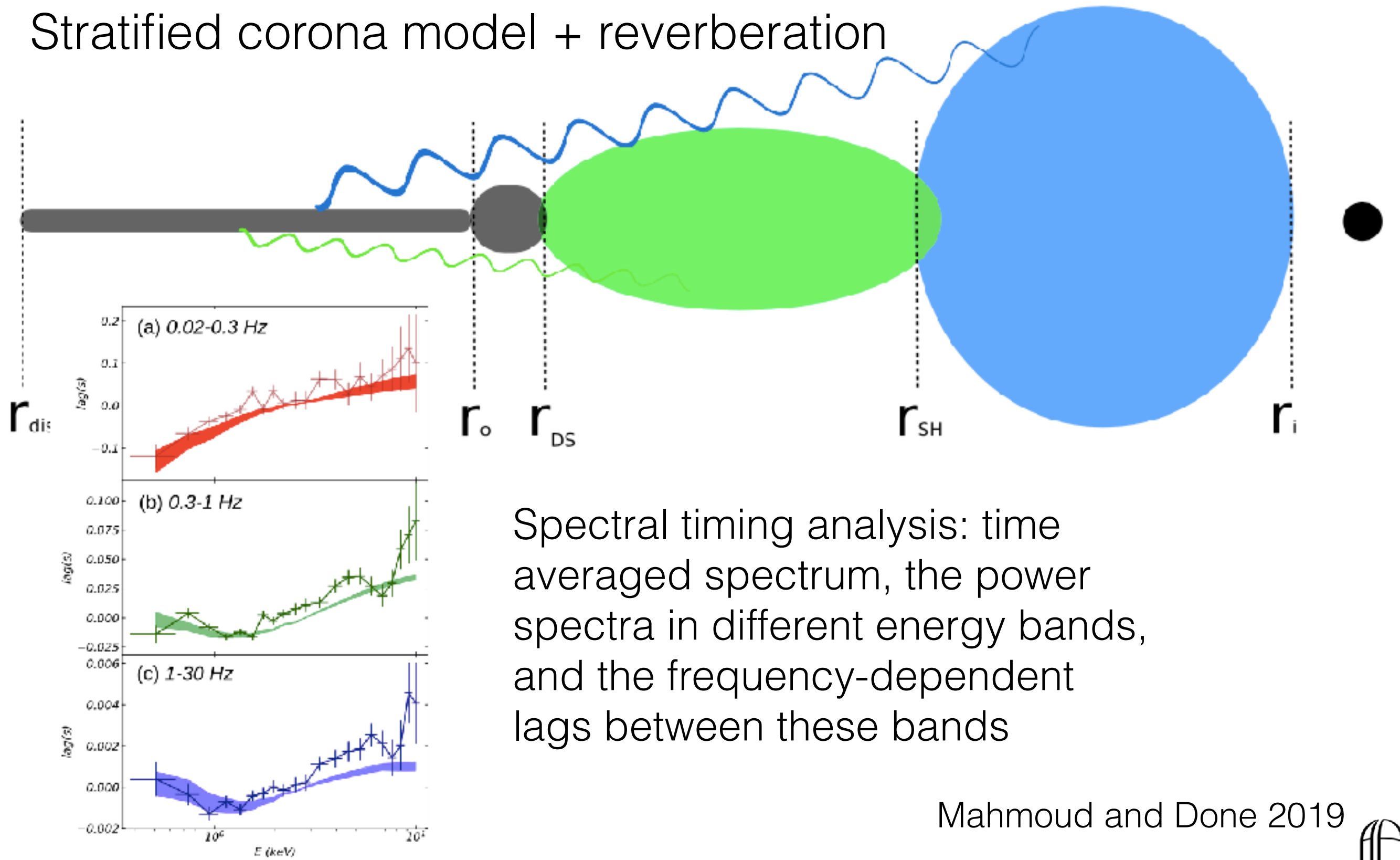
Wilkins+ 2016



ANTON PANNEKOEK
INSTITUTE

Extended Corona

Stratified corona model + reverberation



Mahmoud and Done 2019

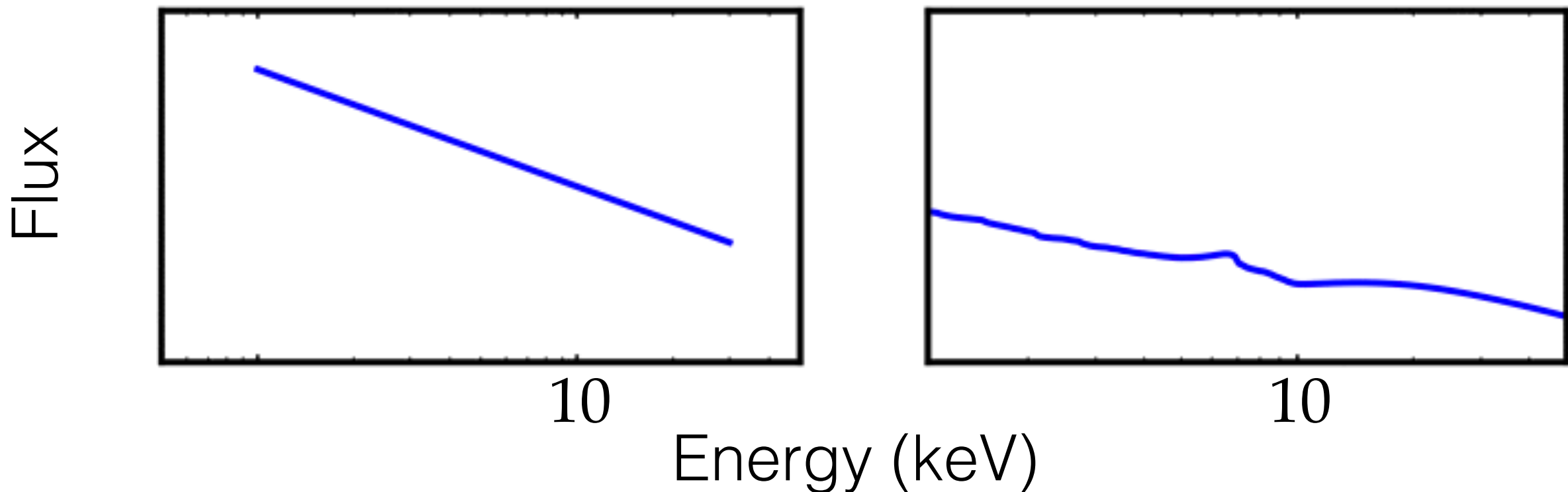


Spectral Hardness Changes

Direct Emission

Reflection

PIVOTING

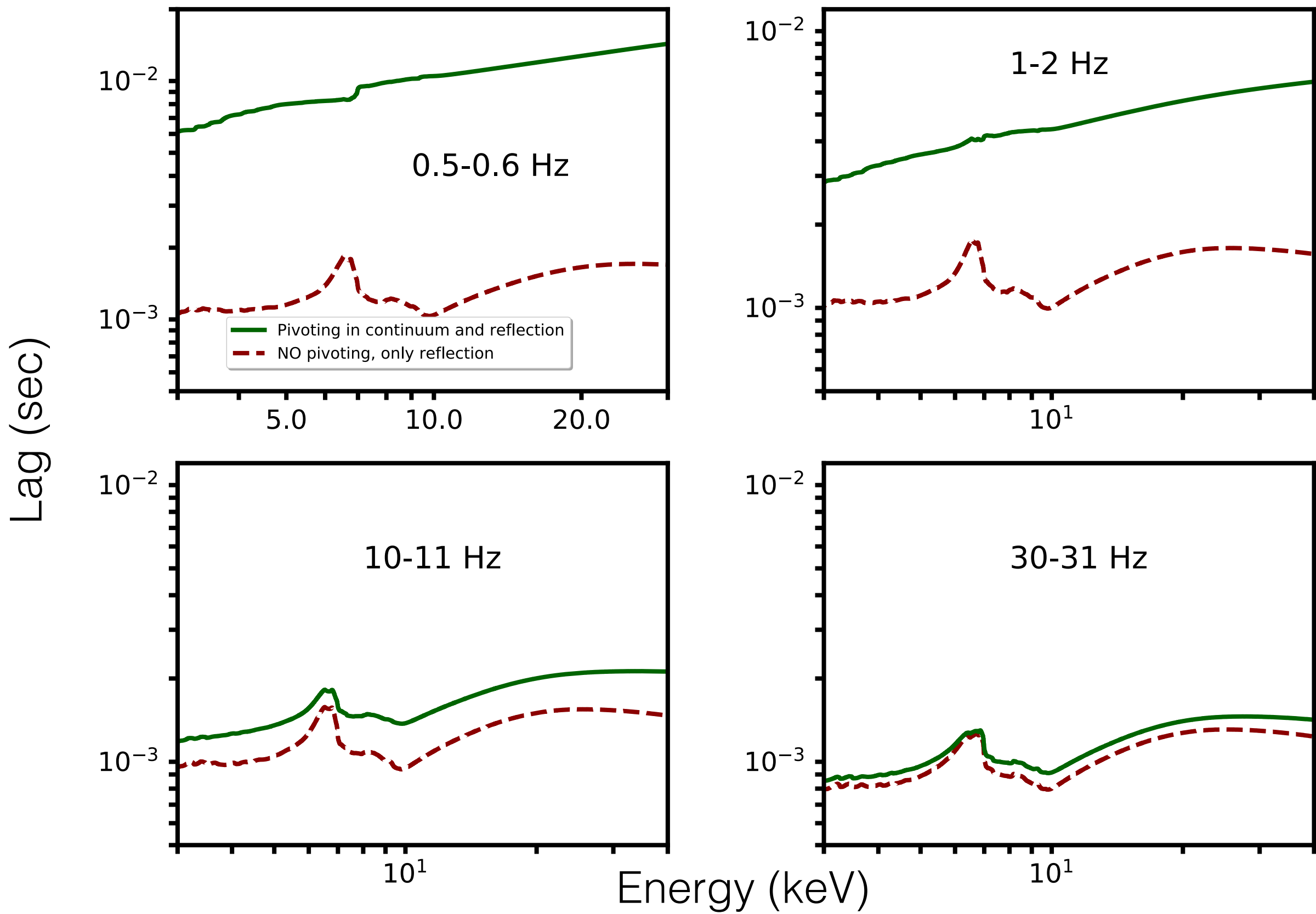


The pivoting power-law produces the hard lags we observed in the data

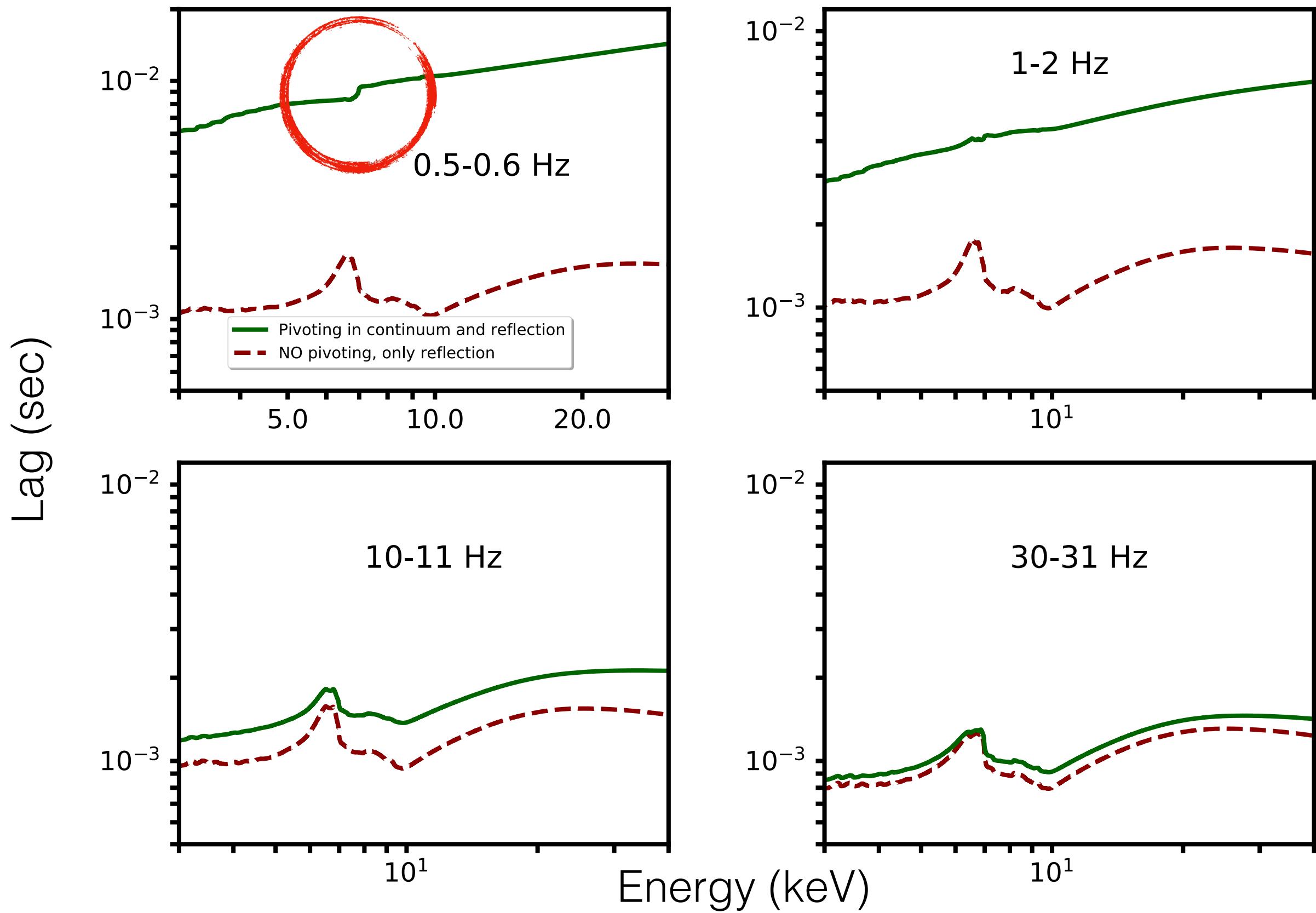
The reflection is changing not only in the slope but also in the atomic physics



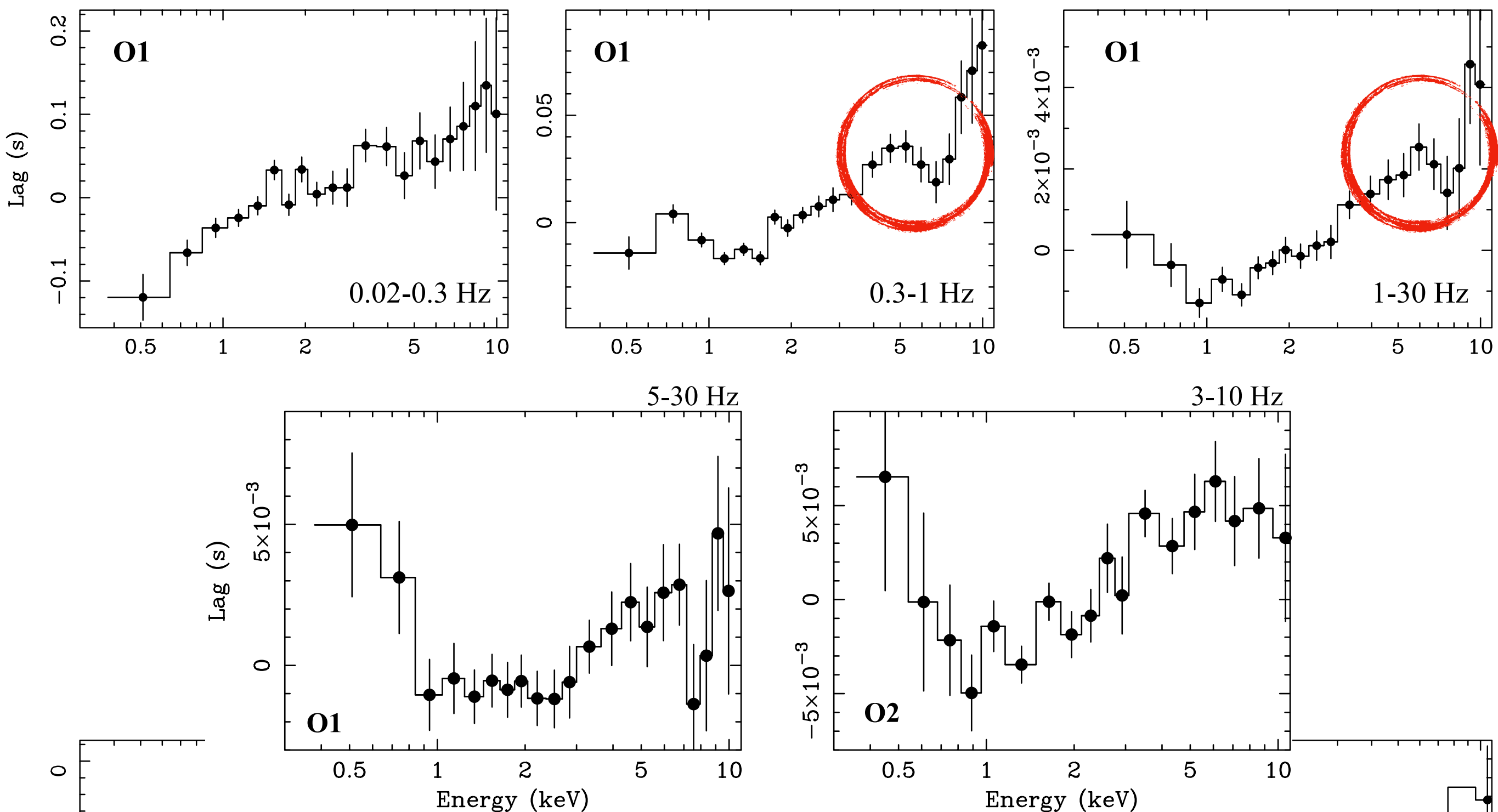
Pivoting Model



Pivoting Model



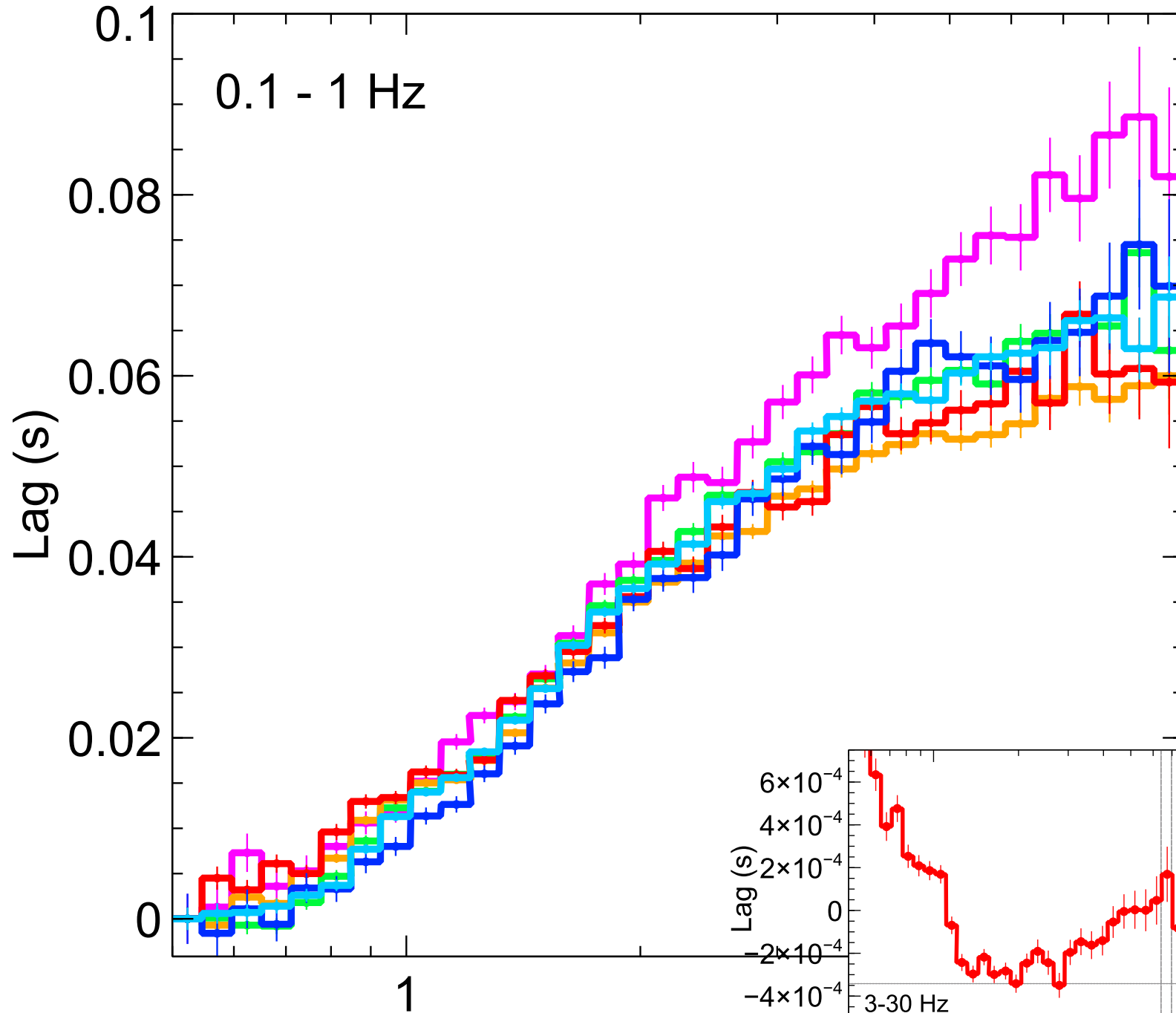
GX 339-4



De Marco+ 2017

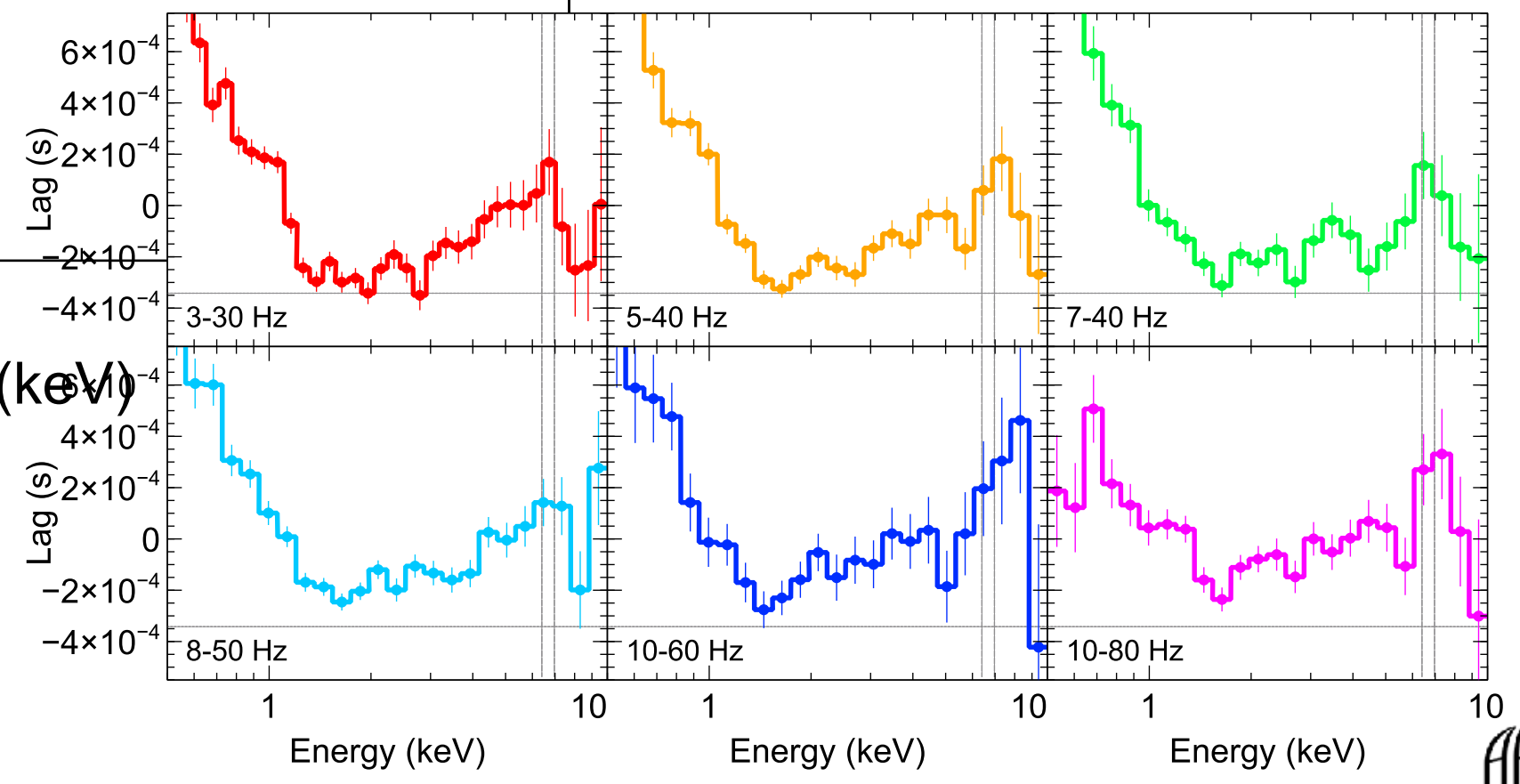


MAXI J1820



0.1 - 1 Hz

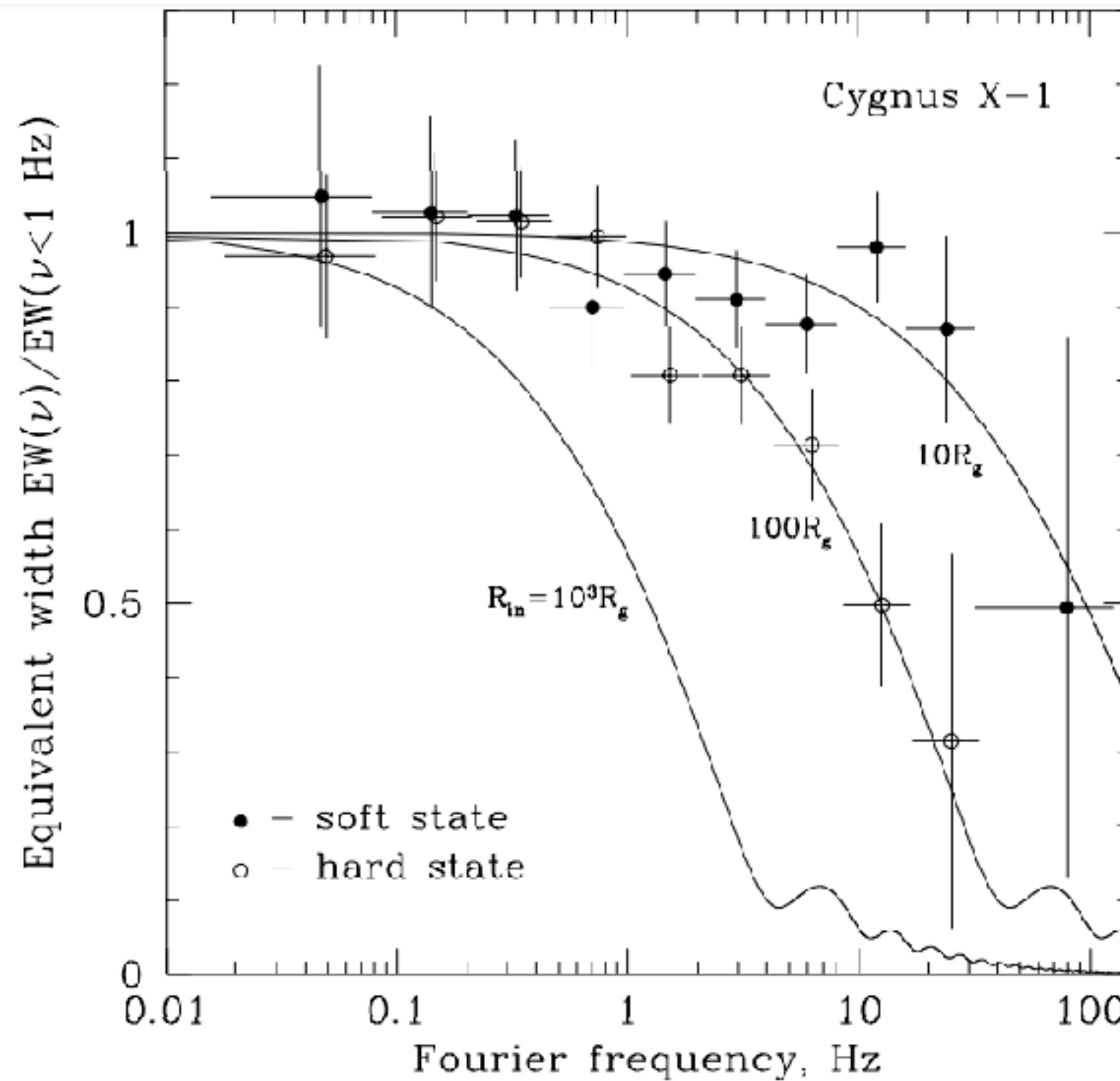
Kara+ 2019



Cygnus X-1

Hard state:
March 1996
(P10238)

Soft state:
June 1996
(P10512)

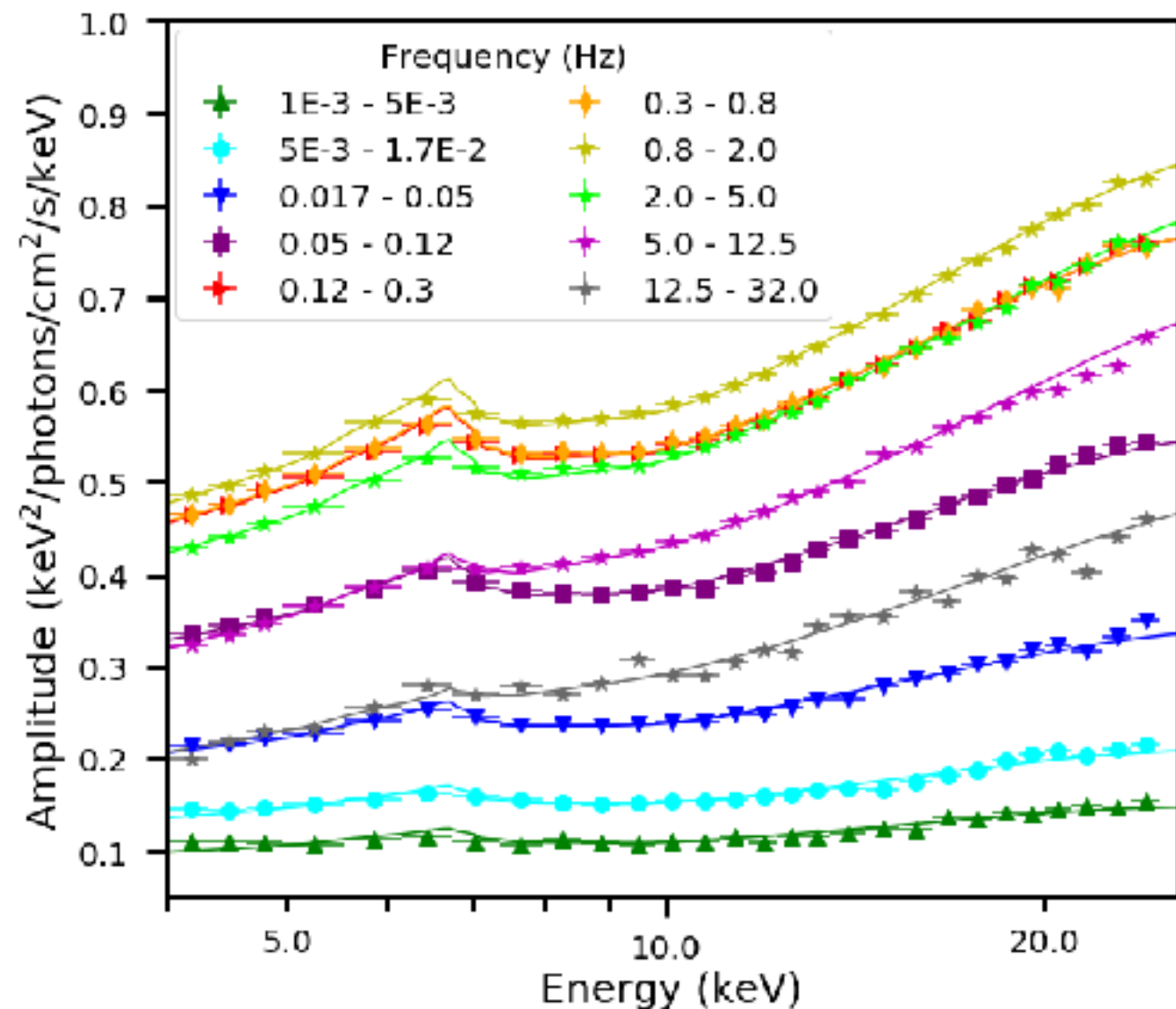
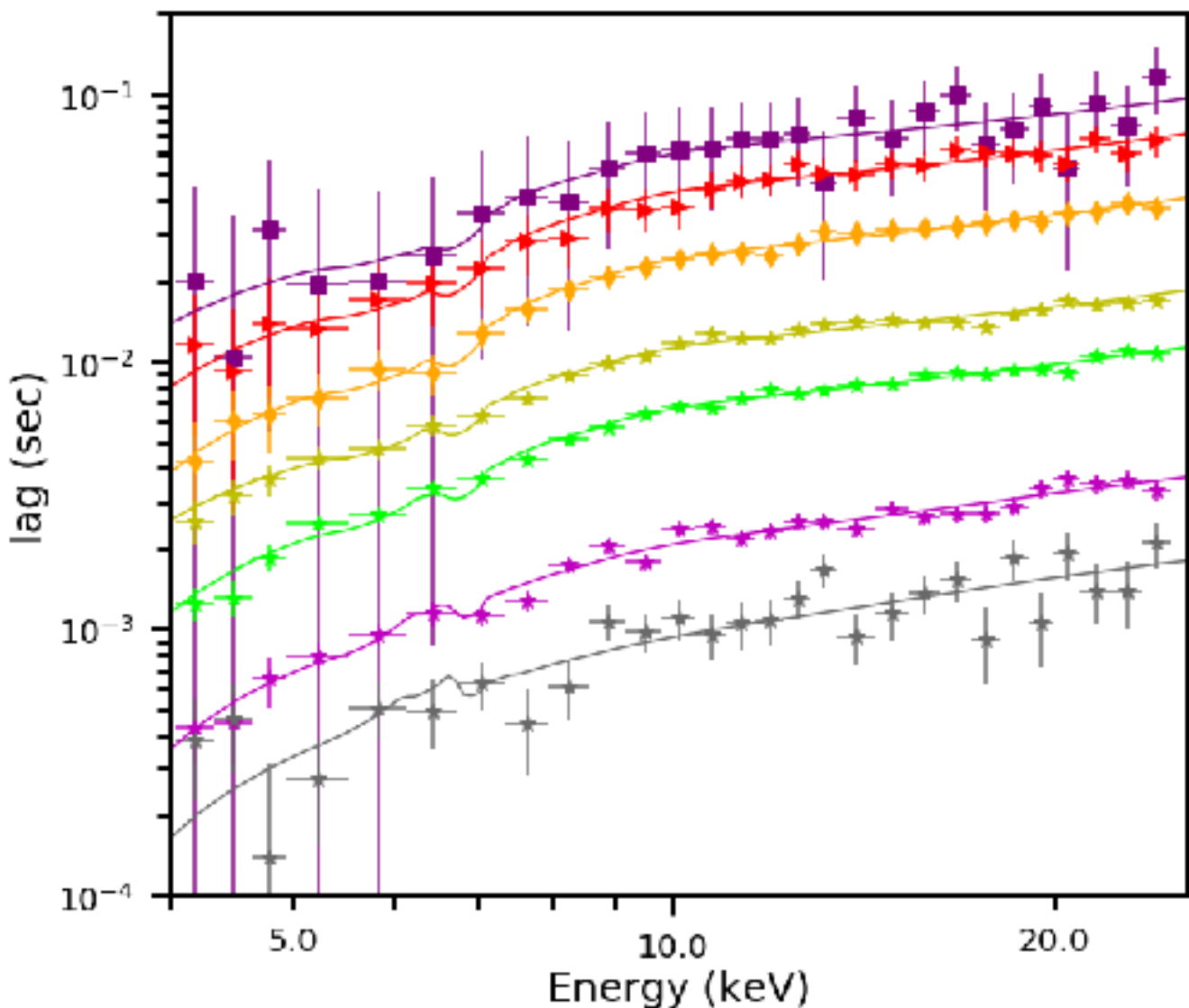


Gilfanov+ 2001



Cygnus X-1

RXTE data set from March 1996 (P10238)
Source in the hard state

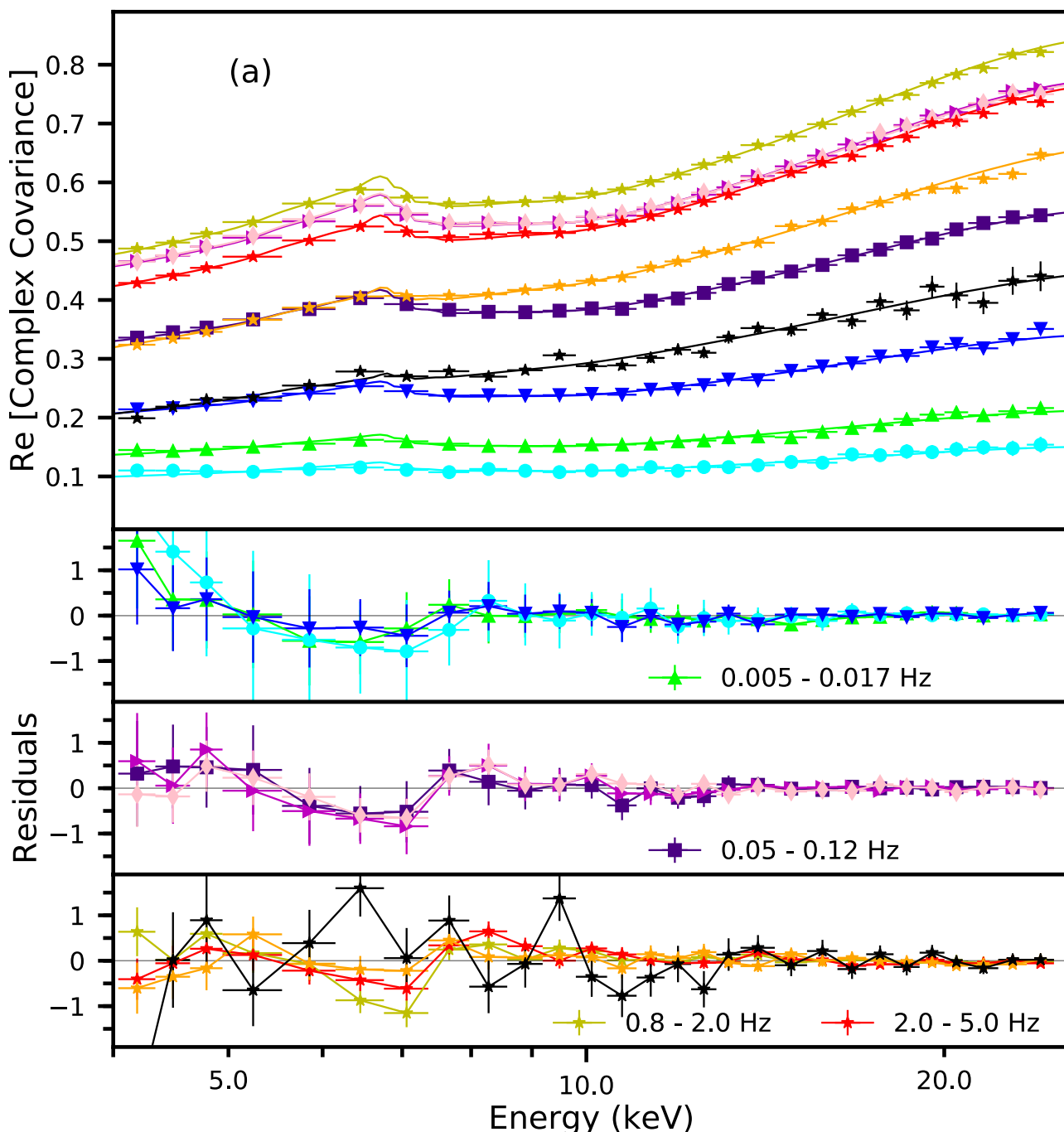


The model reproduce the argument and the amplitude of the cross-spectrum for the Fourier frequencies probed by RXTE

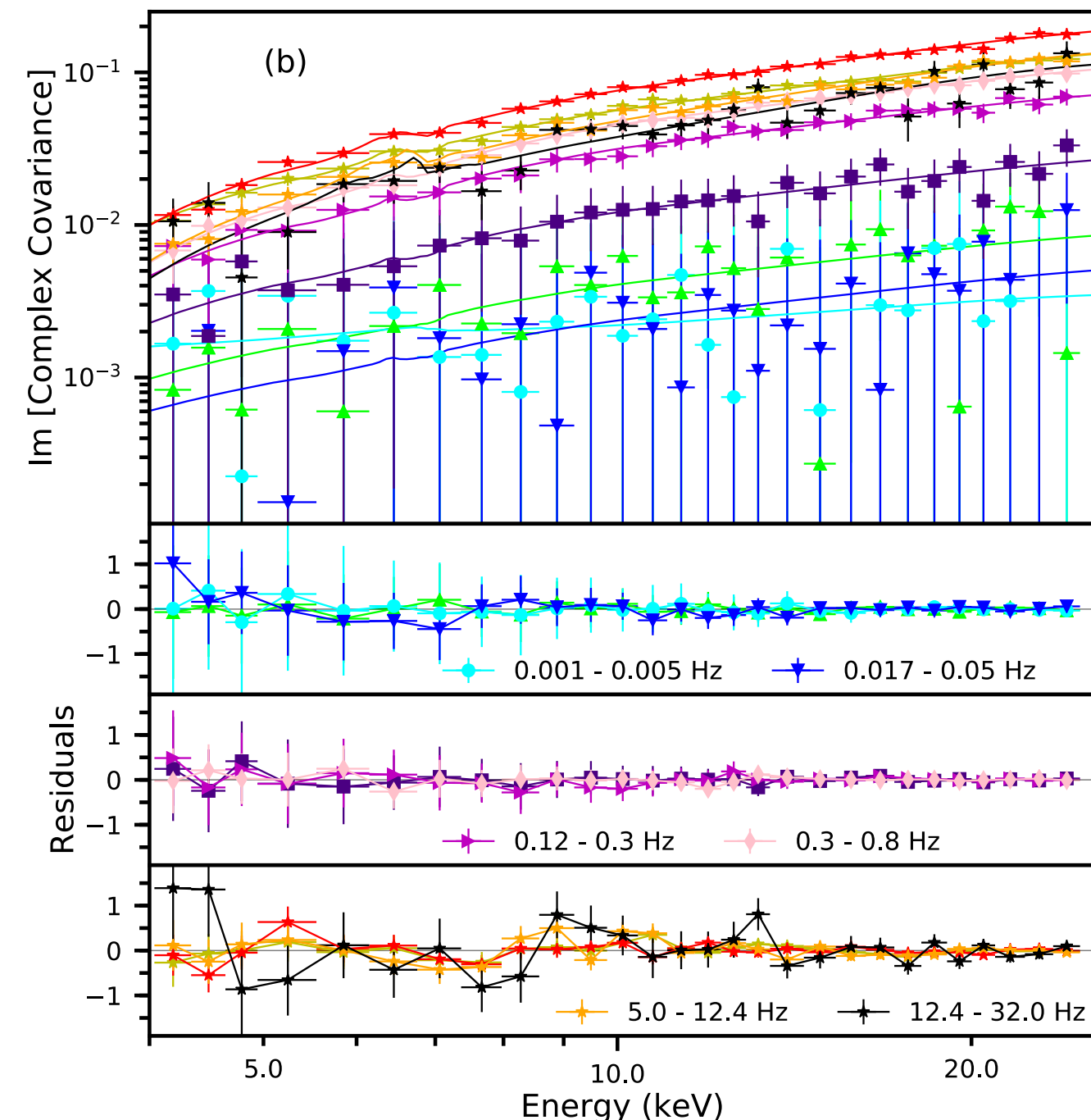


Cygnus X-1 FIT

Real Part



Imaginary Part

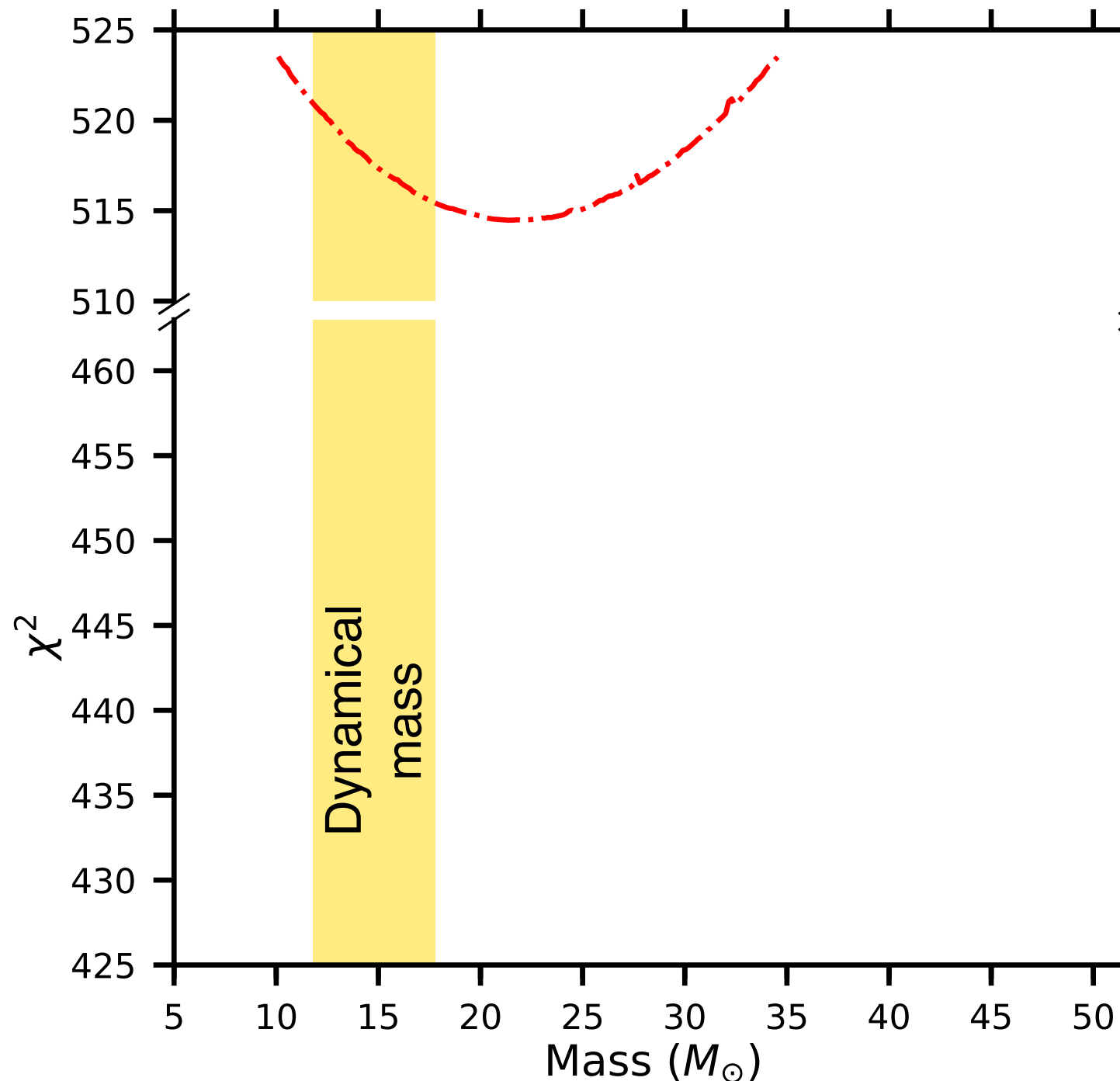


Fit to the data taking into account all the
information of the cross-spectrum



Cygnus X-1

Chi-squared curve of the black hole mass



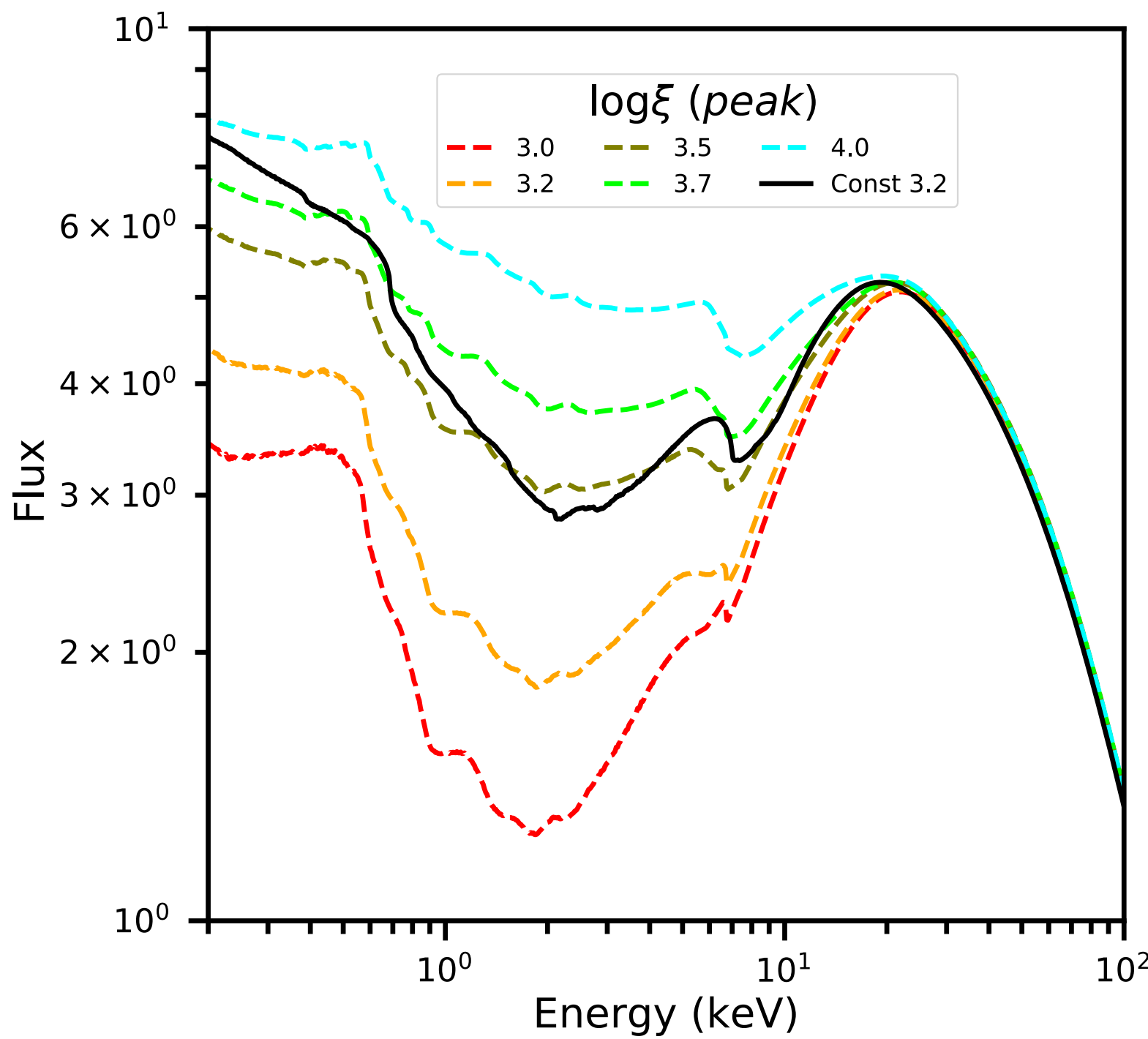
Data set from
1996 RXTE!

The model is sensitive to the mass and can constrain it

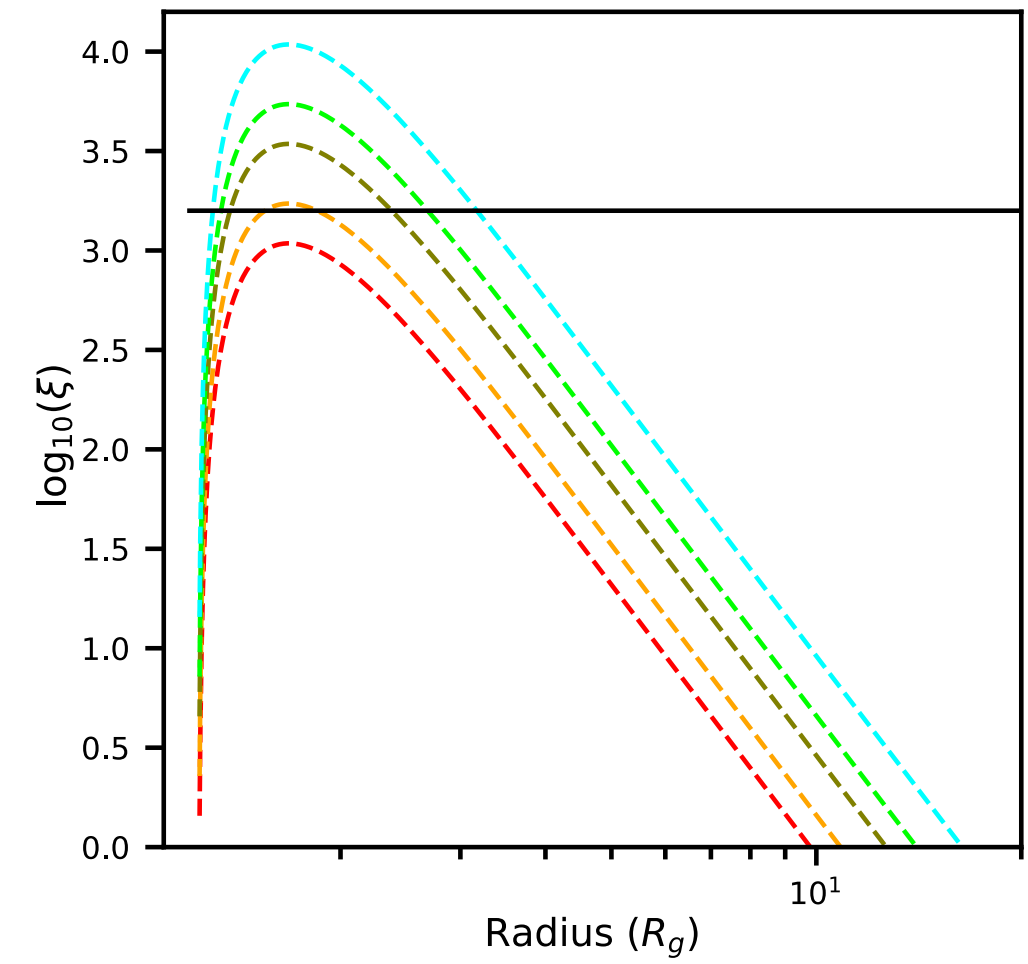


Ionisation profile

Introducing a radial ionisation profile changes the shape of the time-averaged spectrum



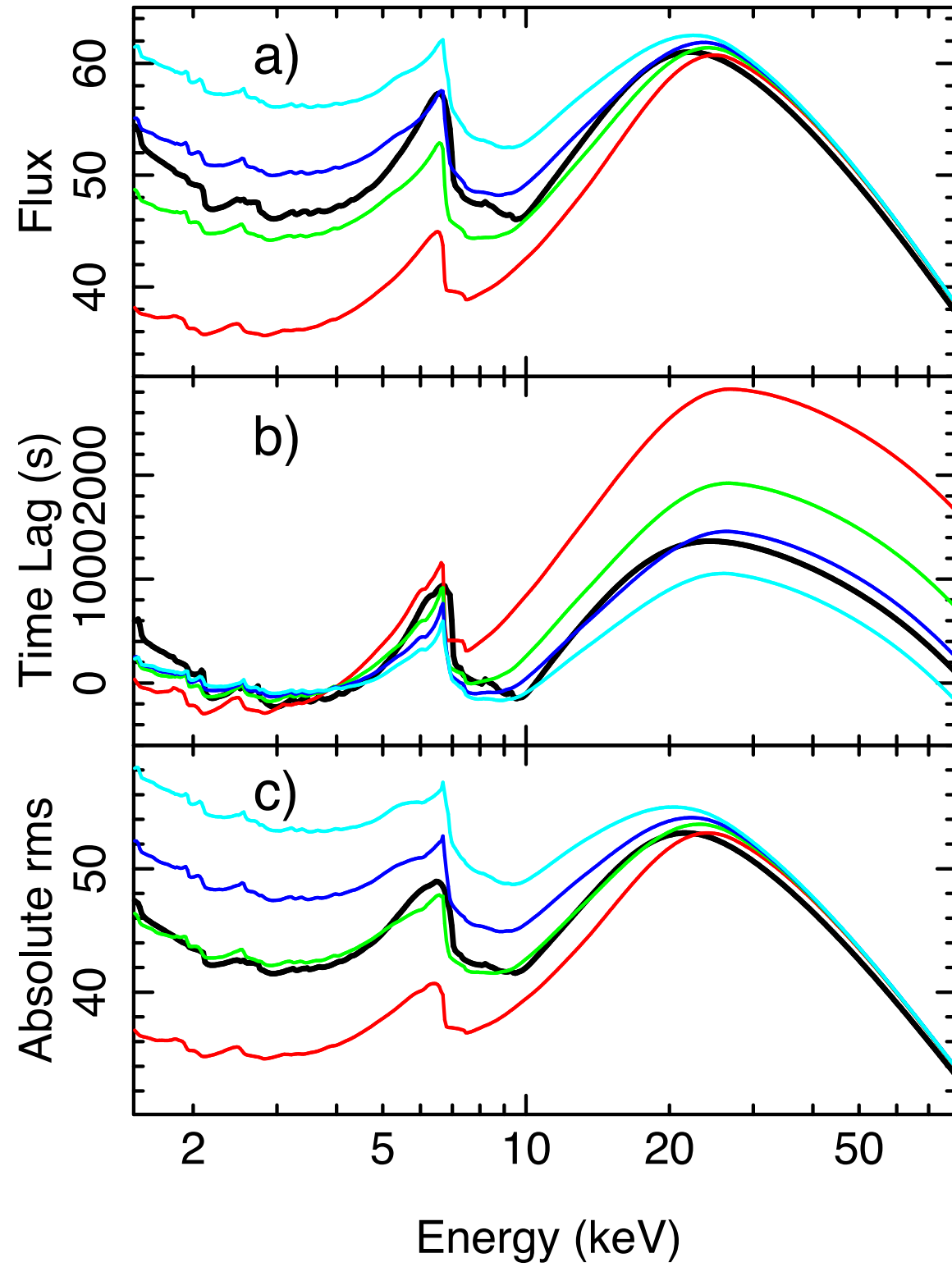
Different radial ionisation profile in the disc



Ingram, Mastroserio+ 2019



Ionisation profile



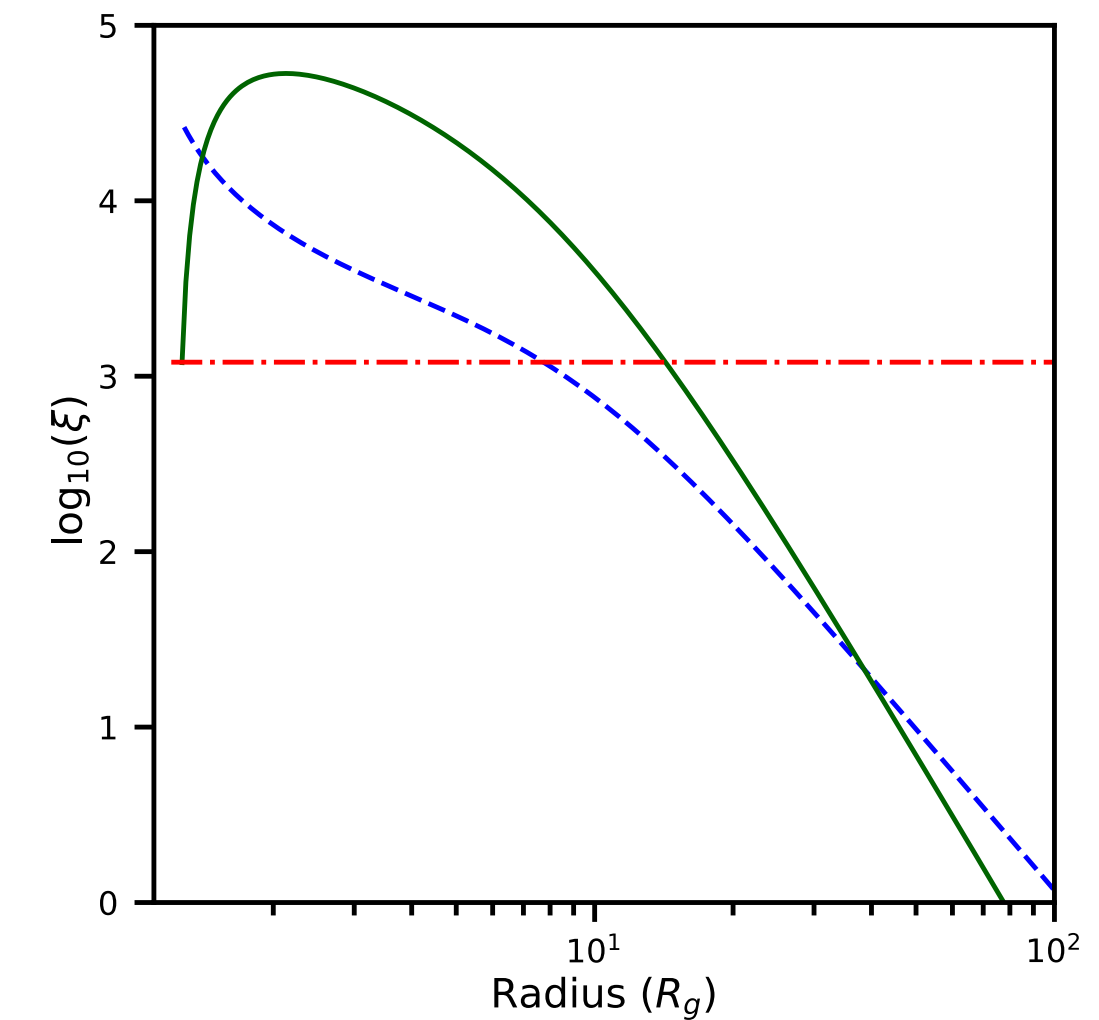
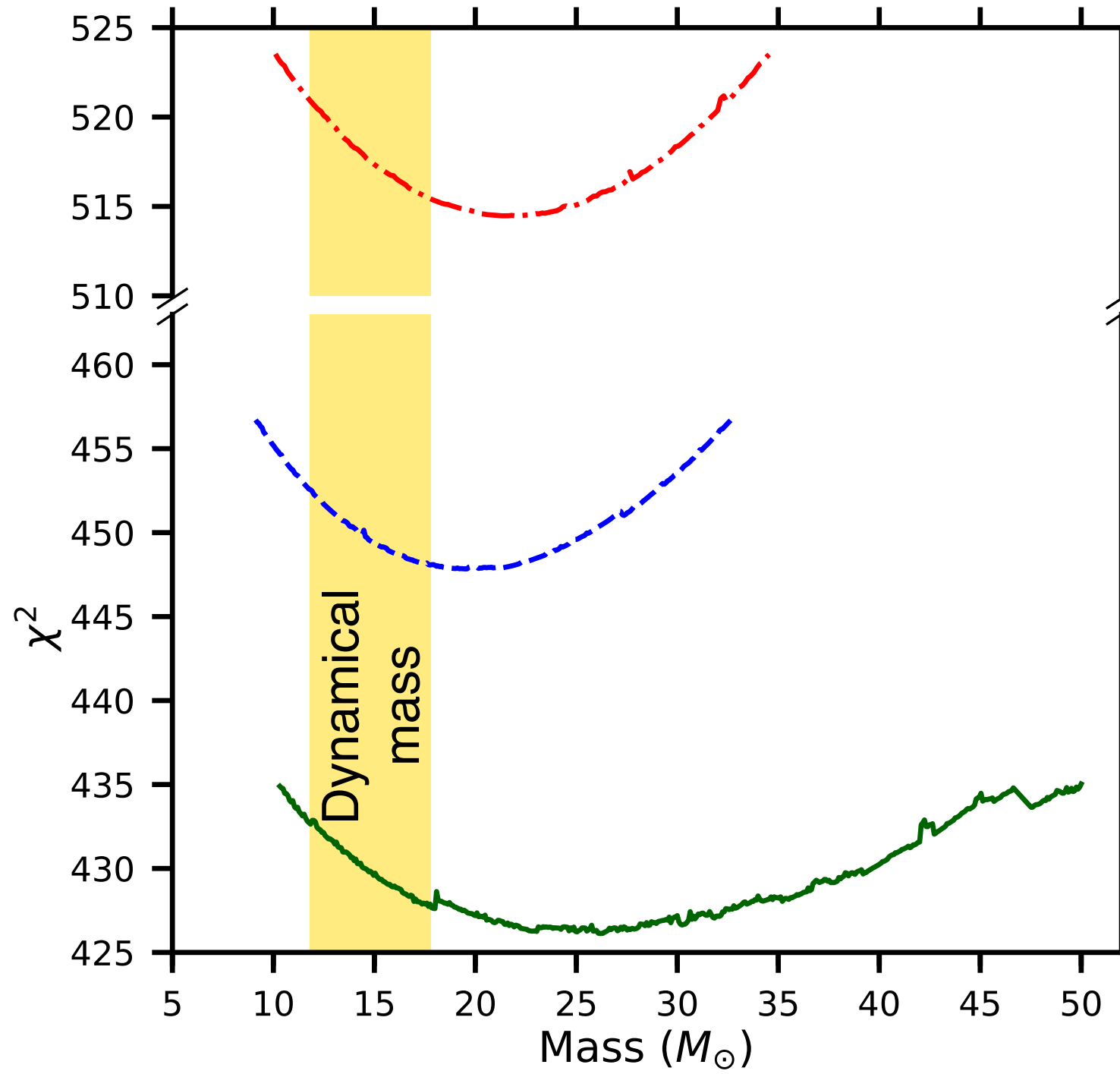
Not constant ionisation changes not only the shape of the time average spectrum but also of both the time lag and the amplitude spectrum

Ingram, Mastroserio+ 2019



Cygnus X-1

Not-constant radial ionisation profiles in the disc improves the fit

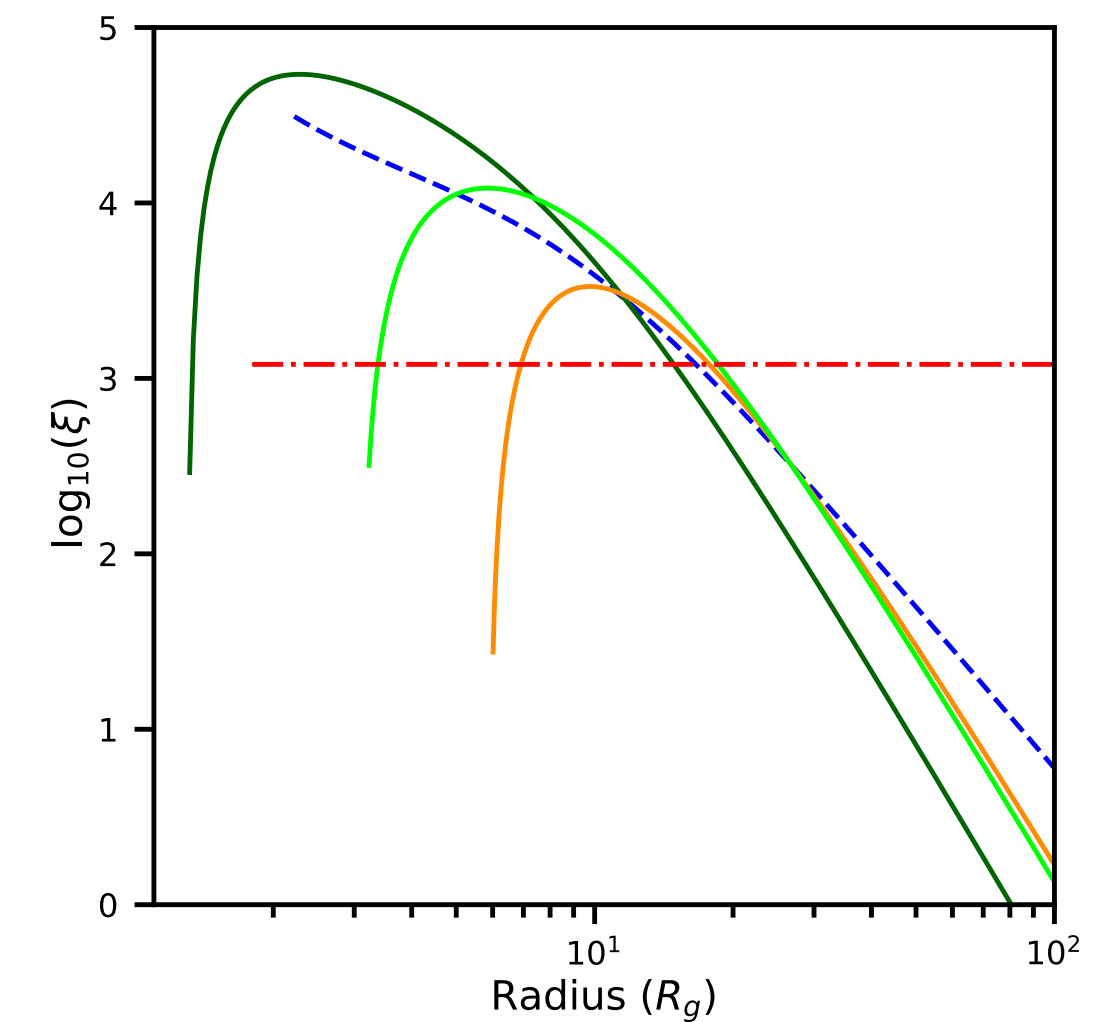
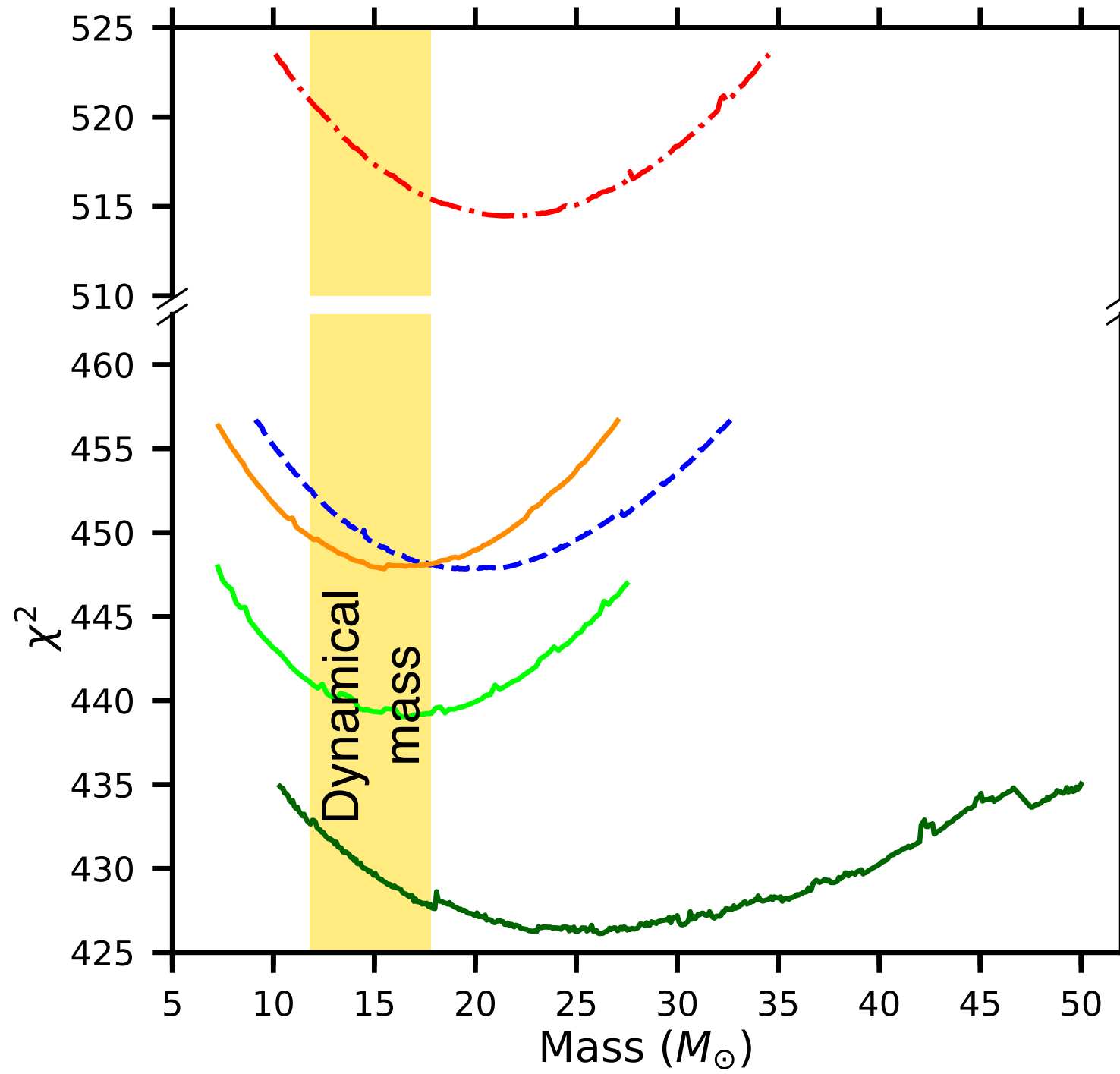


$$\xi = \frac{4\pi F_x}{n_e}$$



Cygnus X-1

We put an upper limit on the peak of the ionisation derived from the lower lower limit on the electron density of the disc



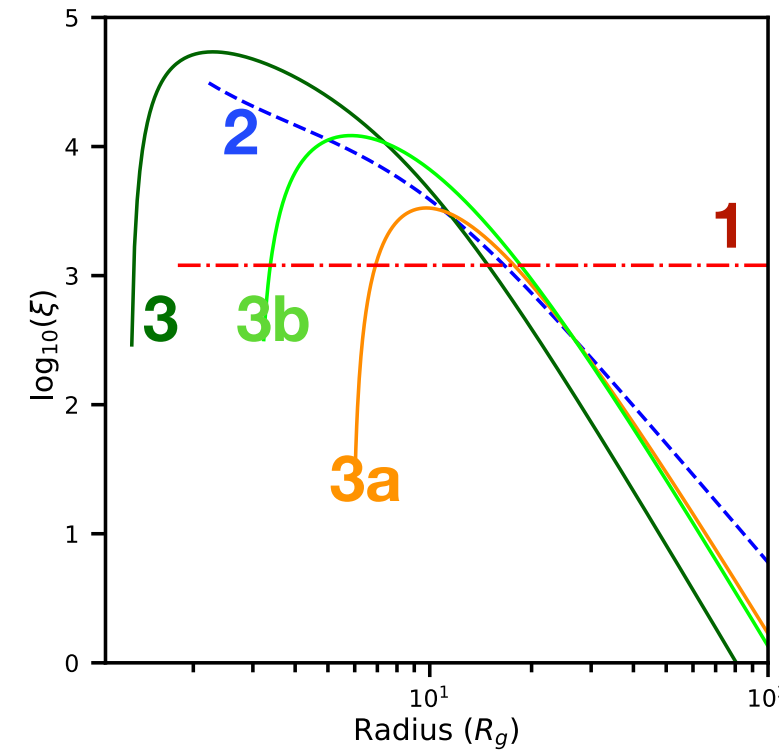
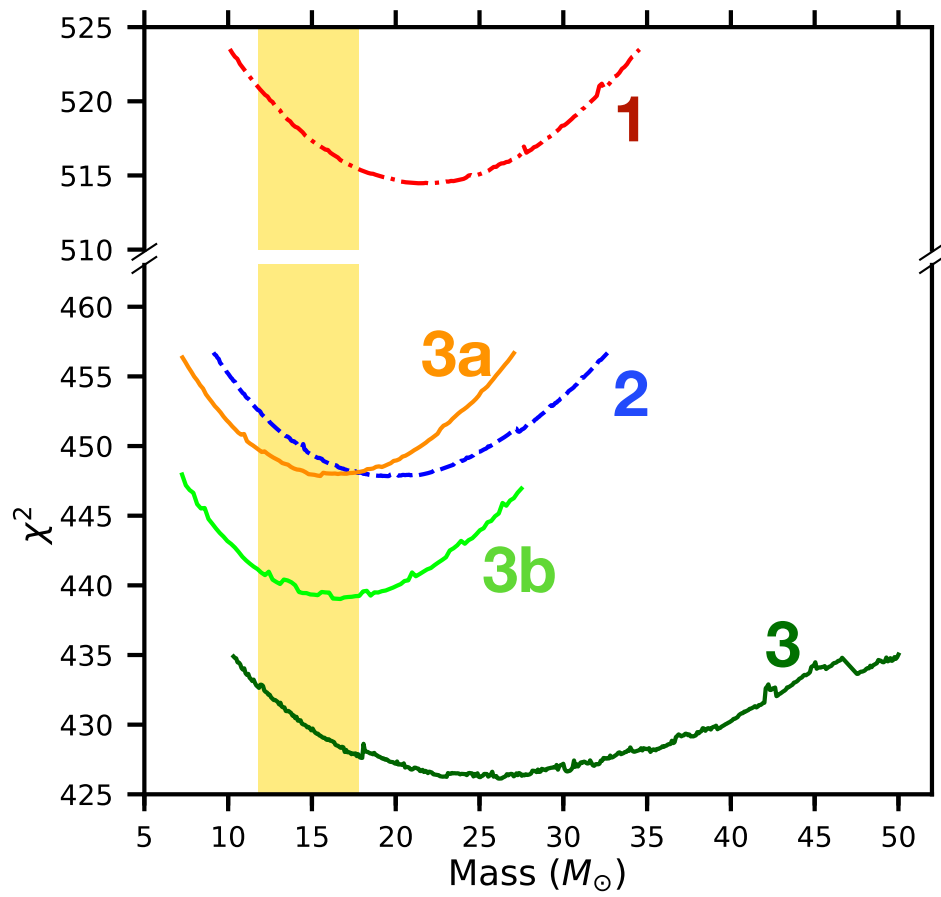
$$\xi = \frac{4\pi F_x}{n_e}$$



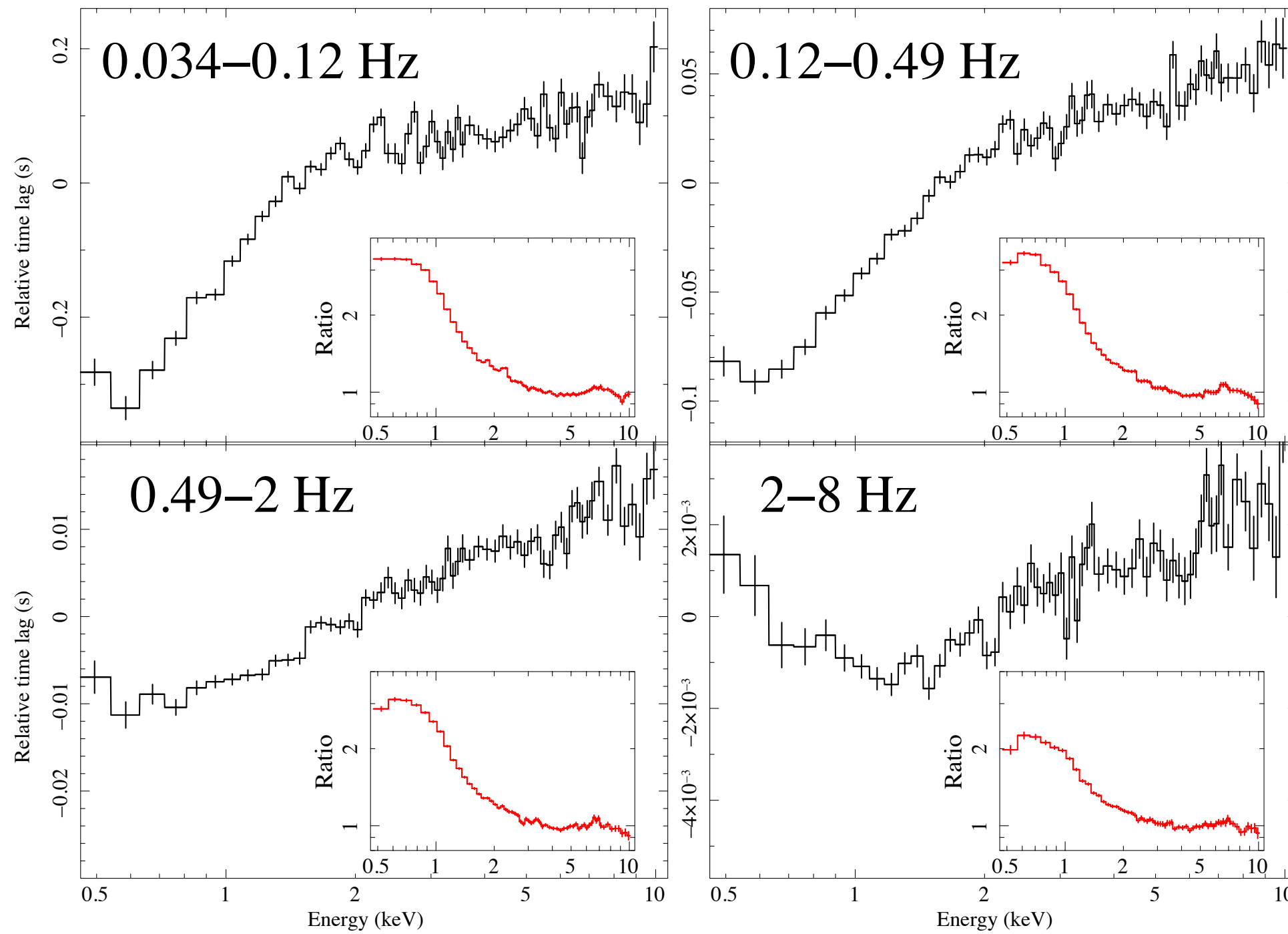
Cygnus X-1

Other results from the fit

	$N_h \left(10^{22} \text{cm}^{-2}\right)$	$h (R_g)$	Incl (deg)	$r_{in} (R_g)$	Γ	$\log \xi^{(a)}$	A_{Fe}	$E_{\text{cut},0} \text{ (keV)}$	Boost	Mass	red χ^2
1)	$0.13^{+0.08}_{-? (b)}$	$6.2^{+0.6}_{-0.8}$	$32.4^{+0.6}_{-1.0}$	$1.8^{+0.4}_{-(c)}$	$1.60^{+0.01}_{-0.01}$	$3.08^{+0.02}_{-0.01}$	$3.7^{+0.1}_{-0.1}$	218^{+13}_{-9}	$0.28^{+0.01}_{-0.01}$	$21.6^{+6.8}_{-6.6}$	515/563
2)	$0.7^{+0.2}_{-0.1}$	$9.7^{+1.9}_{-1.4}$	$33.8^{+1.4}_{-1.5}$	$2.2^{+0.9}_{-1.0}$	$1.65^{+0.02}_{-0.02}$	$4.5^{+0.6}_{-0.7}$	$2.0^{+0.4}_{-0.2}$	371^{+55}_{-63}	$0.50^{+0.05}_{-0.04}$	$19.7^{+5.3}_{-5.4}$	448/563
3)	$0.6^{+0.1}_{-0.1}$	$9.0^{+1.4}_{-1.7}$	$35.0^{+1.2}_{-1.2}$	$1.3^{+0.7}_{-(c)}$	$1.67^{+0.01}_{-0.01}$	$4.7^{+0.7}_{-0.6}$	$1.7^{+0.2}_{-0.3}$	712^{+82}_{-97}	$1.1^{+0.2}_{-0.1}$	$26.0^{+9.6}_{-8.6}$	426/563
3a)	$0.79^{+0.04}_{-0.10}$	$9.5^{+2.7}_{-3.9}$	$35.1^{+1.4}_{-1.0}$	$5.9^{+0.7}_{-0.7}$	$1.67^{+0.01}_{-0.02}$	$3.5^{(d)}$	$1.8^{+0.2}_{-0.1}$	377^{+36}_{-36}	$0.46^{+0.02}_{-0.03}$	$16.5^{+5.0}_{-5.0}$	447/563
3b)	$0.75^{+0.09}_{-0.24}$	$10.8^{+1.9}_{-1.2}$	$35.0^{+0.8}_{-1.8}$	$3.1^{+0.4}_{-0.4}$	$1.66^{+0.02}_{-0.02}$	$4.0^{(d)}$	$1.7^{+0.5}_{-0.3}$	355^{+54}_{-96}	$0.60^{+0.04}_{-0.03}$	$16.5^{+6.1}_{-5.2}$	439/563



Thermal reverberation



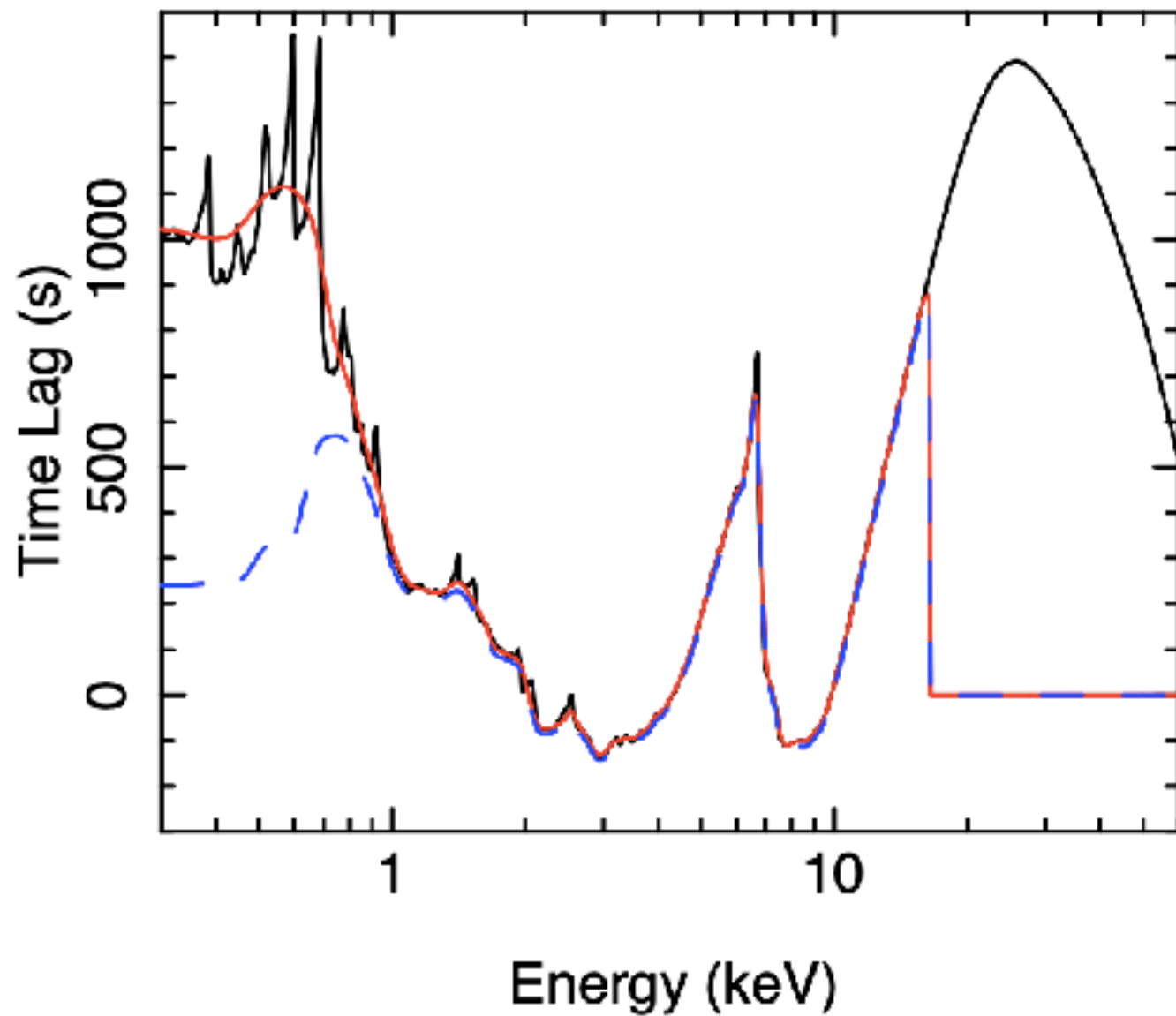
Uttley+ 2014



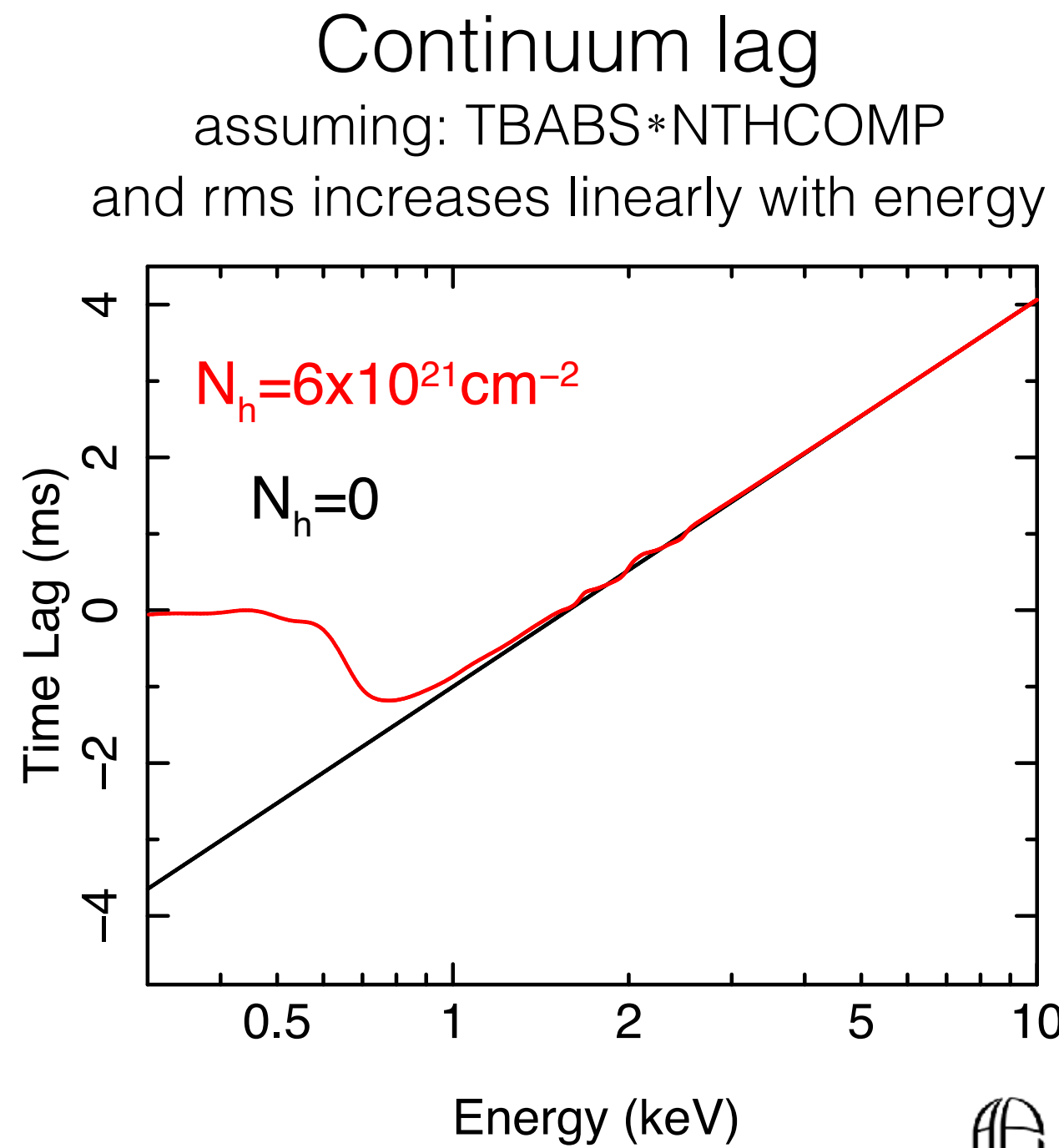
ANTON PANNEKOEK
INSTITUTE

Telescope response

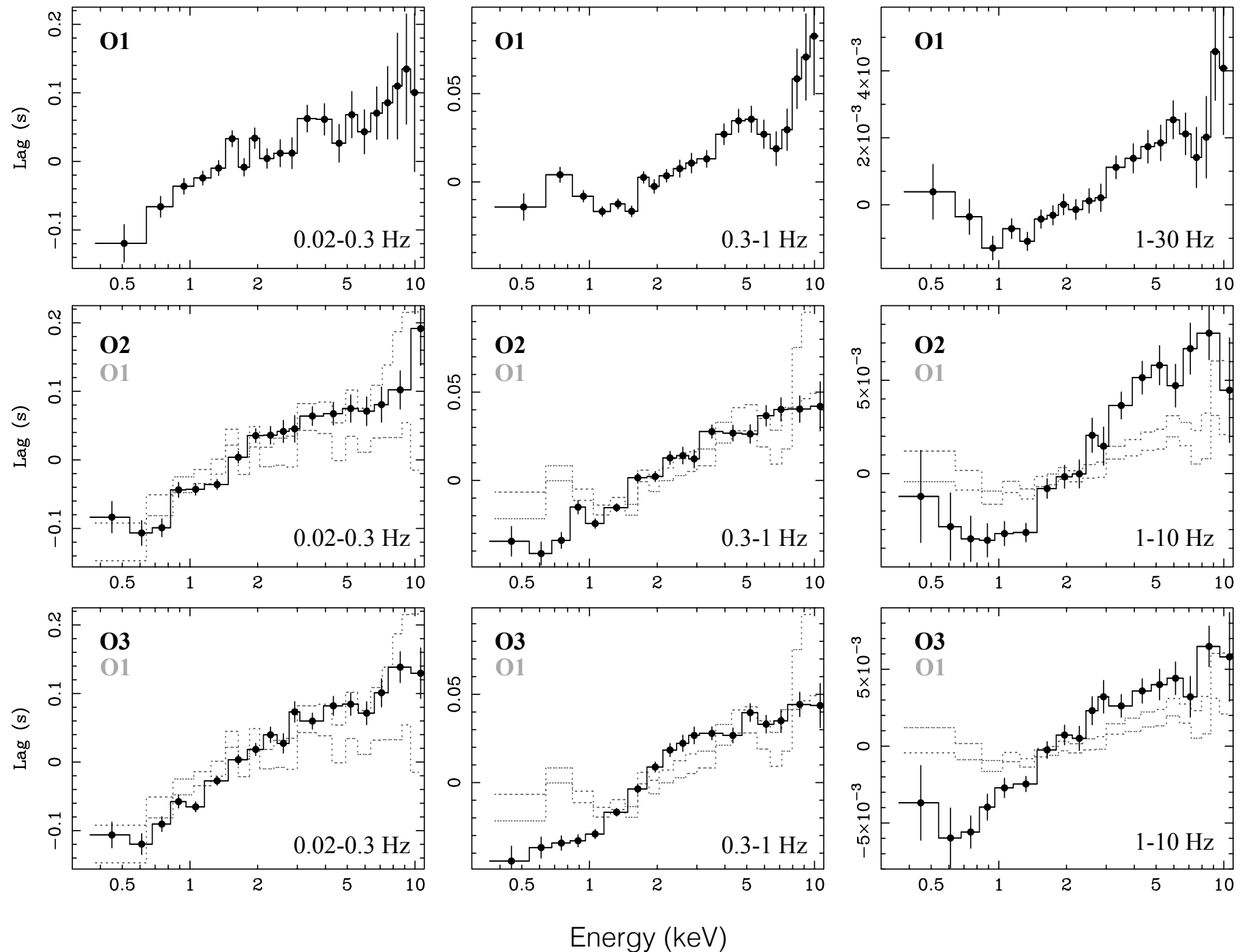
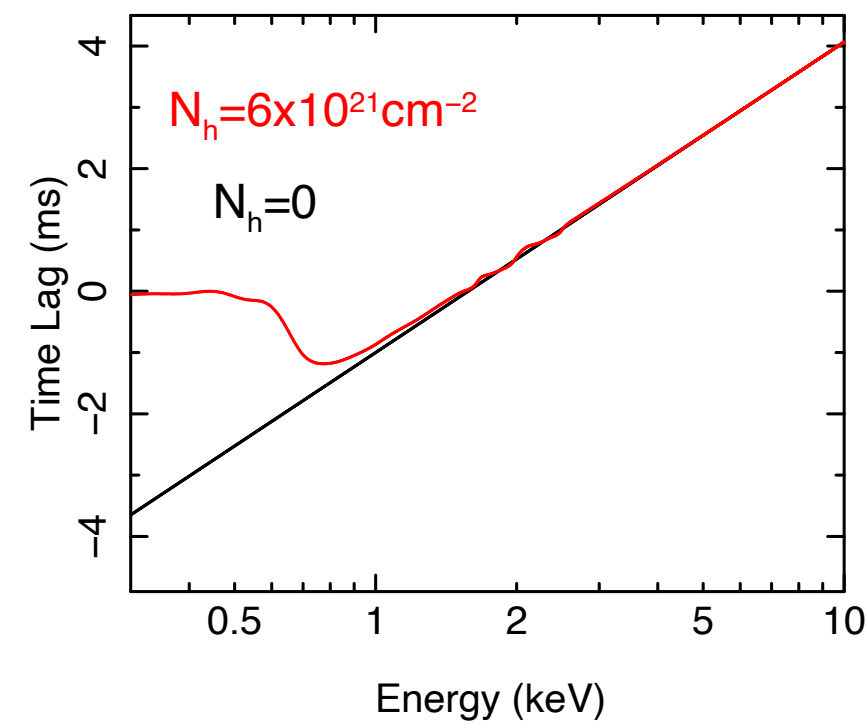
Ignoring the telescope response introduces a bias in the lag spectrum



Reverberation lag

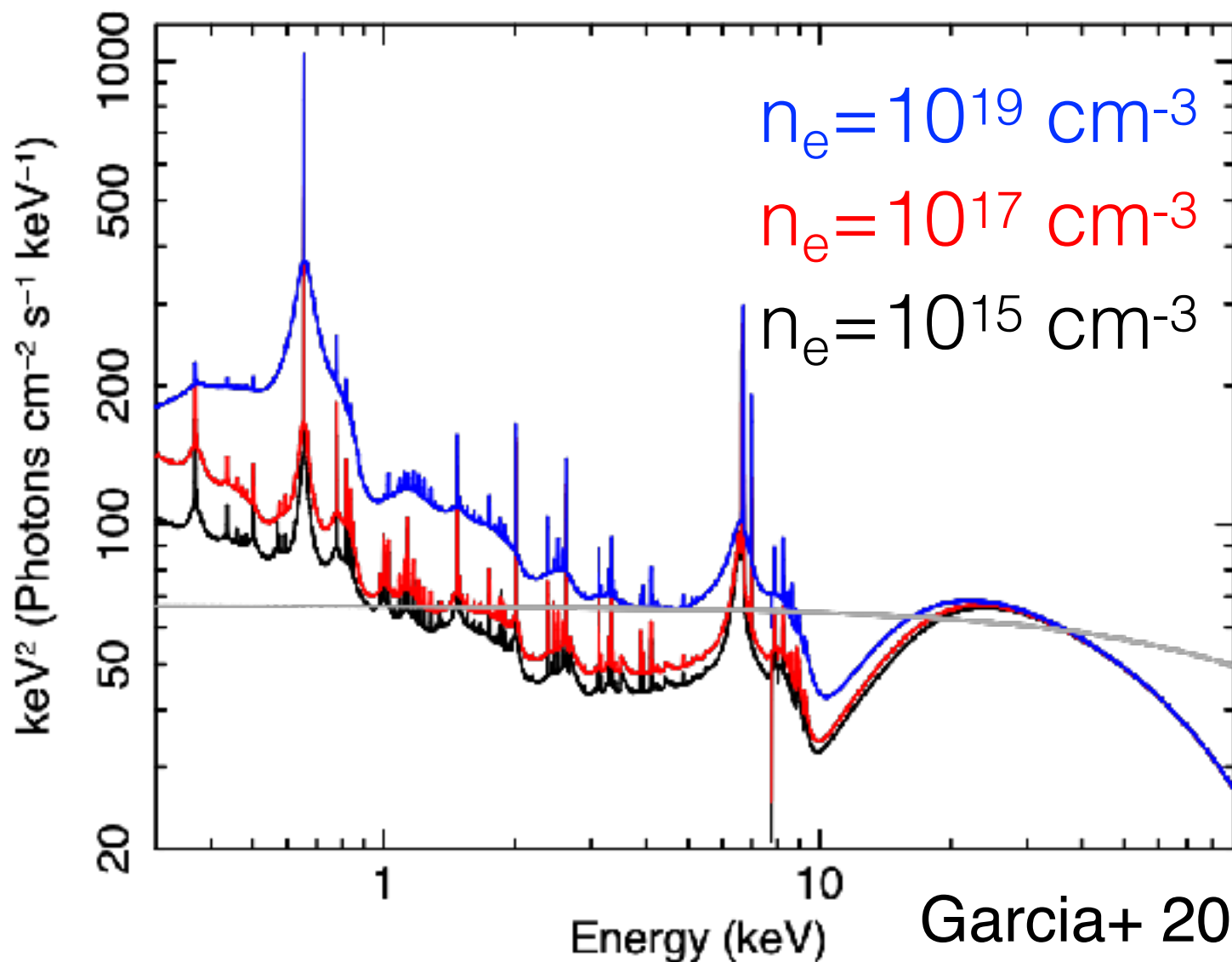


Thermal reverberation



Disc density

Currently using restframe reflation model (xillver)
that assumes $n_e = 10^{15} \text{ cm}^{-3}$

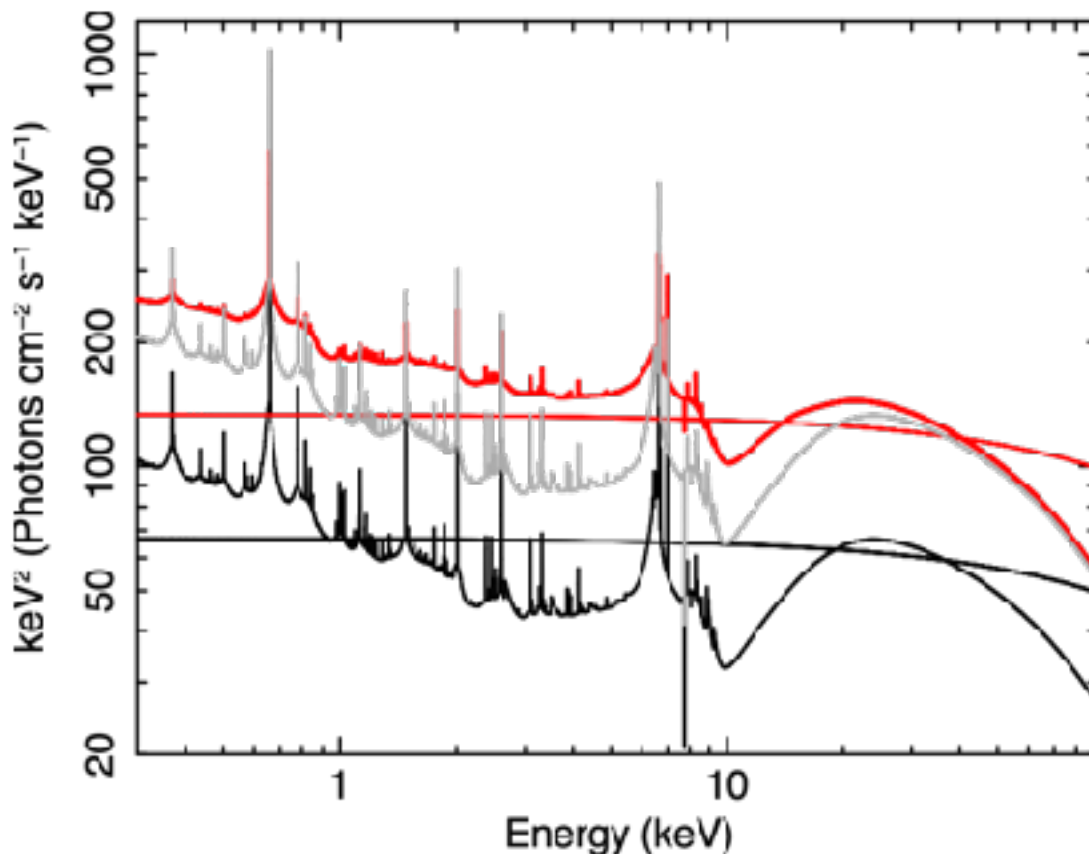


DISC DENSITY

higher density \Rightarrow hotter disc
for same ionisation state \Rightarrow
different reflection spectrum
for same ionisation state

Garcia+ 2016; Tomsick+ 2017; Jiang+ 2019a,b

Thermal reverberation



- Increase continuum flux => increase $\xi = 4\pi F_x / n_e$
- This is never taken into account
- New model will account for this (subtle changes)

